



Cite this: *J. Mater. Chem. A*, 2025, **13**, 27772

## Fundamental concepts of 3,4-alkoxythiophene-based polymeric systems, from synthesis to applications

Francisco A. Bravo-Plascencia,<sup>ab</sup> M. Paola Flores-Morales,<sup>ab</sup> Alexander Kuhn,<sup>ab</sup> Gerardo Salinas<sup>ab</sup> \* and Bernardo A. Frontana-Uribe<sup>ab</sup>

Conducting polymers are one of the most interesting materials due to their broad range of applications, from sensing and energy storage to organic actuators. Among the different conducting polymers, the family of poly-3,4-alkoxy thiophenes stands out due to its exceptional electrical, optical, and chemical properties. The electro-donating effect of the 3,4-alkoxy groups favors the polymerization reaction, provides stereoregularity, and increases the effective conjugation. With poly-3,4-ethylendioxythiophene (PEDOT) as its flagship, this family has gained increasing attention in multiple fields of science, ranging from bioanalysis and electrochromic systems to microelectronics. This review outlines the most recent developments in the study of 3,4-alkoxy thiophenes, from the synthetic routes of monomers to the fundamentals behind the polymerization and functionalization. Finally, conventional and unconventional applications of these materials in different fields of science, *i.e.*, batteries and supercapacitors, electroanalysis, or optoelectronics, are discussed.

Received 21st April 2025  
Accepted 9th July 2025

DOI: 10.1039/d5ta03149d  
[rsc.li/materials-a](http://rsc.li/materials-a)

## Introduction

Since the late 70s, when Shirakawa, MacDiarmid, and Heeger published the first work concerning synthesizing high-conductivity doped polyacetylene, conducting polymers (CPs)

have gained considerable attention in the scientific community.<sup>1-3</sup> From a materials science point of view, CPs have a unique combination of the electrical behavior of metals and the mechanical properties associated with organic polymers. As is well known, the semiconductor behavior of these polymers is based on the redox formation and mobility of charged species within the  $\pi$ -conjugated backbone.<sup>4-7</sup> CPs have passed from a laboratory curiosity to a technological reality due to their numerous applications, ranging from sensing to optoelectronics and energy storage devices.<sup>8</sup> Commonly, many  $\pi$ -conjugated monomers can be used to produce CPs, such as

<sup>a</sup>Instituto de Química, Universidad Nacional Autónoma de México, Circuito Exterior Ciudad Universitaria, CDMX, 04510, Mexico

<sup>b</sup>Centro Conjunto de Investigación en Química Sustentable UAEM-UNAM, Km 14.5 Carretera Toluca-Atlacomulco, Toluca, 5200, Mexico. E-mail: [bafrontu@unam.mx](mailto:bafrontu@unam.mx)

<sup>c</sup>Univ. Bordeaux, CNRS, Bordeaux INP, ISM, F-33607 Pessac, UMR 5255, France. E-mail: [gerardo.salinassanchez@enscbp.fr](mailto:gerardo.salinassanchez@enscbp.fr)



Francisco A. Bravo-Plascencia

*Francisco A. Bravo-Plascencia received his BSc in Chemistry in 2020 from Yachay Tech Experimental Technology University in Ecuador, and in 2023, his MSc degree in Chemical Sciences at the National Autonomous University of Mexico (UNAM) under the supervision of Prof. Bernardo A. Frontana Uribe. His research interests include conducting polymers, electrochemistry for sensing pollutants and organic molecules, as well as the use of green solvents in electrochemistry.*



M. Paola Flores-Morales

*M. Paola Flores-Morales received her BSc in Chemistry from the Autonomous University of the State of México (UAEMéx) in 2024 under the supervision of Prof. Bernardo A. Frontana Uribe. Her undergraduate research focused on the electro-synthesis of conducting polymers from thiophenic derivatives in green solvent Cyrene®. Her academic interests include sustainable chemistry, electroactive materials, and computational approaches in chemistry.*



aniline, pyrrole, furan, or thiophene. In particular, thiophene-based polymers exhibit high chemical and electrochemical stability, which is attributed to the stabilizing effect of the positive charges by the sulfur heteroatom and the resonance effect within the conjugated oligomer.<sup>9</sup> Furthermore, incorporating electron-donating substituents onto positions 3 and 4 of the thiophene ring favours the electropolymerization mechanism, stabilizes the formed radical cations, and minimizes  $\alpha$ - $\beta$  and  $\beta$ - $\beta$  couplings of the oligomers. Consequently, poly-3,4-dialkoxythiophenes have become one of the most studied materials in the field of CPs, and numerous potential applications have been developed.<sup>10-12</sup> The poly-3,4-dialkoxythiophene family has a good balance between conductivity, stability, and processability, making their materials very attractive among



Prof Dr Alexander Kuhn

Society, and Fellow of the International Society of Electrochemistry. He is the recipient of several honors, including the Grand Prix Sûe of the French Chemical Society and the CNRS science medal in silver.



Dr Gerardo Salinas

electrochemistry-based light emitting devices, and magnetoelectrochemistry.

*Prof Dr Alexander Kuhn obtained his Master's in chemistry from TU Munich, and his PhD from the University of Bordeaux. After his post-doc at Caltech, he moved back to Bordeaux, where he is currently a Full Professor in chemistry. He is also an Adjunct Professor at VISTEC, Thailand, Distinguished Professor at Henan University, China, senior member of the Institut Universitaire de France, distinguished senior member of the French Chemical*

*Dr. Gerardo Salinas received his Master's and PhD degrees in electrochemistry from the National Autonomous University of Mexico (UNAM). Since 2018 he has been performing postdoctoral studies at the Institute of Molecular Sciences (ISM) at the University of Bordeaux (France) under the supervision of Prof. Alexander Kuhn. His research interests include bipolar electrochemistry, conducting polymers, electrochemistry-based light emitting devices, and magnetoelectrochemistry.*

different families of CPs (Table 1). This review provides a complete overview of recent trends in the study and applications of poly-3,4-dialkoxythiophenes. At first, different synthetic routes for the efficient design of 3,4-dialkoxythiophene monomeric derivatives and the possible chemical modification of the conjugated ring are summarized. Afterwards, chemical and electrochemical polymerization methods of the monomers and the formation of copolymers are discussed. Finally, the current state of the art of selected applications of these  $\pi$ -conjugated systems is presented.

## Synthesis of 3,4-alkoxy thiophene-based monomers

The most well-established methodology for synthesizing 3,4-dialkoxythiophenes is based on a four-step reaction route (Scheme 1). At first, a Hinsberg condensation between the thioglycolic acid ester (1) and an  $\alpha$ -dicarbonyl (2a, b) in the presence of a strong base, *i.e.*, sodium methoxide, generates the corresponding 3,4-dihydroxythiophene-2,5-dialkyl ether (3), which is the starting molecule for the synthesis of 3,4-alkoxythiophenes.<sup>13-15</sup> After this, the Williamson etherification of (3) with alkyl halides in the presence of  $K_2CO_3$  leads to O-alkylation at the 3,4-position, producing the 3,4-alkoxythiophene-2,5-dialkyl ether (4a-g).<sup>16</sup> In the next step, 3,4-alkoxythiophene-2,5-dicarboxyl acid (5) is formed *via* a simple saponification reaction, and finally, the Cu-catalyzed proto decarboxylation in quinoline leads to the synthesis of the desired 3,4-alkoxythiophene (6).<sup>17</sup> Although, as mentioned above, this is the most common methodology for synthesizing 3,4-alkoxythiophenes, multiple variations of each reaction step have been developed.<sup>18-20</sup> This section summarizes different synthetic approaches explored to improve each reaction step involved in the synthetic route to obtain 3,4-alkoxy thiophenes.



Prof Dr Bernardo A. Frontana-Uribe

*Prof Dr Bernardo A. Frontana-Uribe obtained his BSc in Chemistry (1989-1993) and MSc in Organic Chemistry (1993-1995) at the Faculty of Chemistry-UNAM Mexico. He carried out his doctoral studies at the University of Rennes I in France (1995-1999) in electrosynthesis of heterocyclic compounds. Later, he did postdoctoral work at the University of Freiburg, Germany, in electrosynthesis of thiophenic conductive polymers with Prof Jürgen Heinze. Thereafter, he joined the Institute of Chemistry of UNAM to create the laboratory of Electrochemistry and Electrosynthesis. His research interests include conducting polymers, organic electrosynthesis methodology, natural product electrotransformations, and electrochemical water treatment process.*



Table 1 Property comparison between different families of conducting polymers<sup>275</sup>

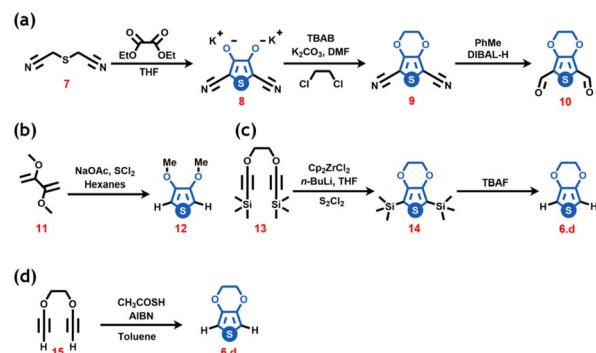
Polymer family	Conductivity (S cm <sup>-1</sup> )	Stability	Processability
Polyacetylene	10 <sup>5</sup> (Doped state)	Very poor	Very poor
Polypyrroles	1–100	Poor	Poor
Polyanilines	1–100	Fair	Moderate
Polythiophenes	10 <sup>-3</sup> –10 <sup>2</sup>	Good	Poor
Poly-3,4-dialkoxythiophenes	10 <sup>-3</sup> –10 <sup>2</sup>	Excellent	Excellent

### Thiophene moiety generation

Alternative chemical pathways to the previously described Hinsberg condensation have been developed. For example, Al-jumaili *et al.* modified the classic condensation protocol by using 2,2-thiodiacetonitrile (7) as the starting compound instead of thioglycolic acid, producing 3,4-ethylenedioxothiophene-2,5-dicarbonitrile (9) as an intermediate to access the corresponding aldehyde (10) as the final compound (Scheme 2a).<sup>21</sup> Moreover, Hellberg *et al.* reported a one-step synthesis approach for the synthesis of 3,4-dimethoxythiophene (12) based on a ring closure (addition–elimination) between 2,3-dimethoxy-1,3-butadiene (11) and sulphur dichloride (Scheme 2b).<sup>22</sup> In an alternative approach, a two-step route for the synthesis of 3,4-ethylenedioxothiophene (EDOT) (6d) was developed based on the cyclization reaction of a diyne precursor (13), mediated by di(cyclopentadienyl)zirconium(IV) dichloride ( $Cp_2ZrCl_2$ ) and using disulphuric dichloride as a sulphur source, to generate 2,5-bis(trimethylsilyl)-3,4-ethylenedioxothiophene (14) (Scheme 2c).<sup>23</sup> Afterward, EDOT was obtained through a proto-desilylation in the presence of tetra-*n*-butylammonium fluoride. Finally, a radical-cascade procedure was proposed to synthesize EDOT, in which the thioacetic acid reacts with a diyne precursor (15) in the presence of AIBN acting as the initiator.<sup>24</sup>

### O-Alkylation of the thiophene ring from 3,4-positions

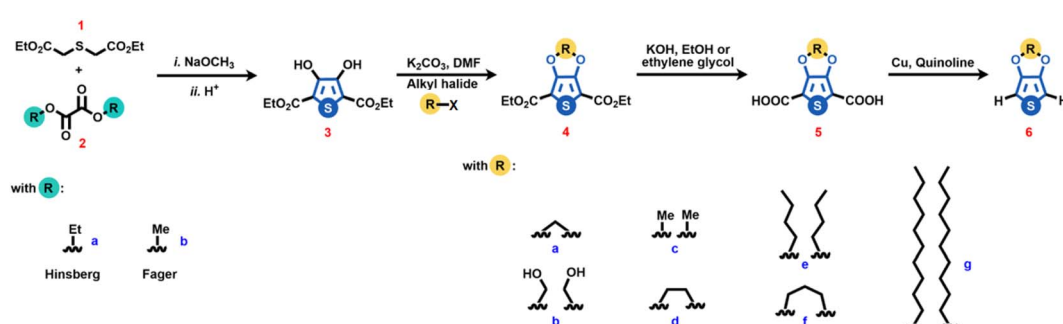
From a synthetic point of view, the *O*-alkylation of (3) or 3,4-dimethoxythiophene is a crucial reaction for synthesizing novel and more sophisticated 3,4-alkoxythiophenes. Three synthetic routes have been developed: the Mitsunobu reaction, a transesterification synthesis, and a double Williamson etherification. The Mitsunobu reaction is based on the use of diethyl



Scheme 2 Synthesis of the thiophene ring to prepare 3,4-alkoxythiophenes; (a) modified Hinsberg condensation, (b) one-step synthesis based on a ring closure (addition–elimination), (c) two-step route based on the cyclization reaction of a diyne precursor and a proto-desilylation reaction, and (d) a radical-cascade synthetic route.

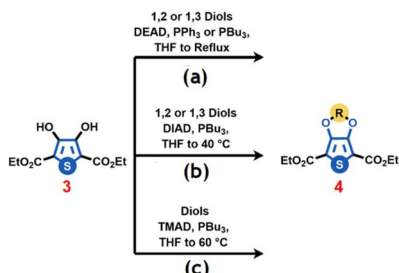
azodicarboxylate (DEAD),<sup>25</sup> dialkylazodicarboxylate (DIAD)<sup>26,27</sup> or tetramethylazodicarboxamide (TMAD),<sup>28,29</sup> acting as a dehydrogenating agent in the presence of tri-substituted phosphine and 1,2- or 1,3-diols (Scheme 3a). This approach has been used for the synthesis of multiple 3,4-alkoxythiophenes, from classic EDOT and 3,4-propylenedioxothiophene (ProDoT) derivatives to more sophisticated alkyl short and large ring-alkylene, benzyl, or crown ether-like thiophenes.

Transesterification is a reaction between an ether and an alcohol, catalyzed by an acid, to interchange functional groups. Such a reaction has been extended to the *O*-alkylation of 3,4-dimethoxythiophene, acting as a starting compound.<sup>30</sup> For example, Krishnamoorthy *et al.* used dibenzyl and substituted phenylene 1,3-diols to synthesize dibenzyl propylenedioxothiophene and 3,4-phenylenedioxothiophene derivatives



Scheme 1 Classic four-step reaction route for the synthesis of substituted 3,4-dialkoxythiophenes.

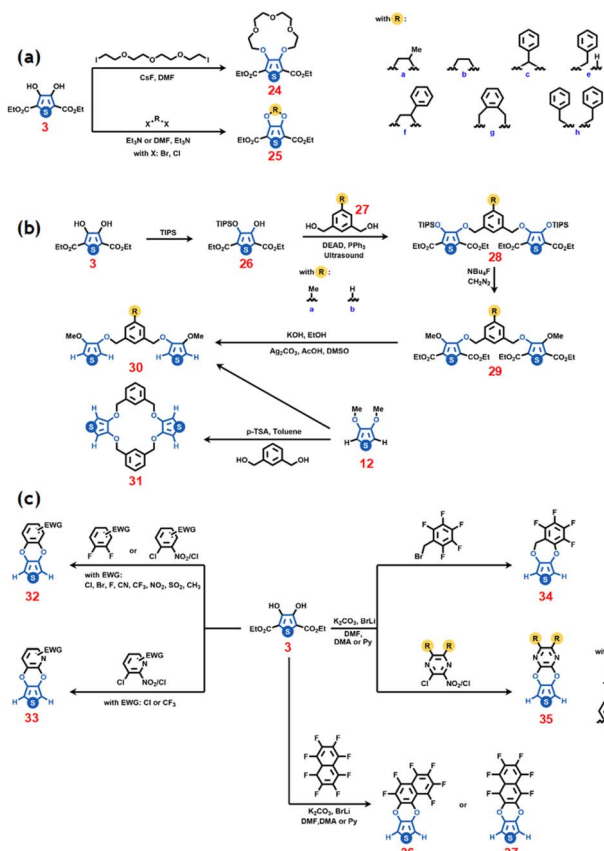




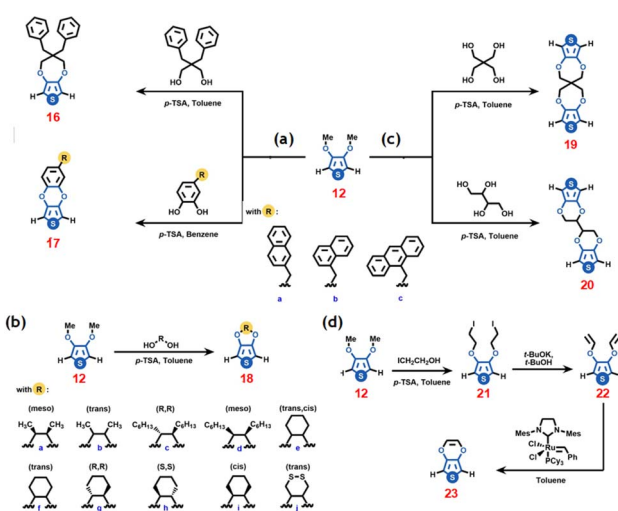
**Scheme 3** *O*-alkylation of 3,4-dialcoxythiophenes based on the Mitsunobu reaction using (a) diethyl azodicarboxylate (DEAD), (b) di-alkylazodicarboxylate (DIAD) and (c) tetramethylazodicarboxamide (TMAD) as dehydrogenating agents.

(Scheme 4a).<sup>31,32</sup> In addition, with this methodology, enantio-merically pure chiral EDOT derivatives have been designed (Scheme 4b).<sup>30,33</sup> Furthermore, a double transesterification of the four positions of pentaerythritol with two 3,4-dimethoxythiophene molecules was reported to produce the spiro bipropylenedioxothiophene (19) (Scheme 4c).<sup>34</sup> The same approach was used to synthesize bis-EDOT by using threitol as a bridge to connect two EDOT moieties.<sup>35</sup> On the other hand, using the acid transesterification reaction, it is possible to produce interesting reactive 3,4-dialkoxythiophene intermediaries such as 3,4-diiodoethoxythiophene. Roncali *et al.* exploited the reactivity of such a molecule to synthesize 3,4-vinylenedioxothiophene (VDOT) (23) (Scheme 4d).<sup>36</sup> A continuous flow synthesis process of 3,4-propylenedioxothiophene derivatives is based on this methodology.<sup>37</sup>

The double Williamson etherification reaction has recently garnered considerable attention due to the potential *O*-alkylation of (3) with high steric hindrance substituents (Scheme 5a). The ring closure step is achieved using alkyl halides and trialkyl



**Scheme 5** *O*-alkylation based on a double Williamson etherification reaction for the synthesis of (a) 3,4-alkoxythiophenes with high steric hindrance substituents (b) macrocycle 3,4-alkoxythiophenes and (c) 3,4-phenylenedioxothiophene (PhEDOT) functionalized with electron-withdrawing groups.



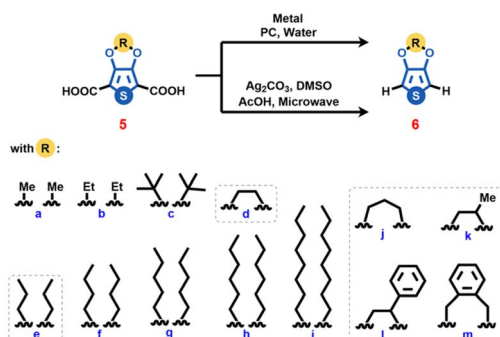
**Scheme 4** *O*-alkylation based on a transesterification reaction for the synthesis of (a) dibenzyl propylenedioxothiophene and 3,4-phenylenedioxothiophene derivatives, (b) chiral EDOT derivatives, (c) bis-alkoxythiophenes and (d) 3,4-vinylenedioxothiophene (VDOT).

amines, acting as substituent moieties and a base-solvent.<sup>38</sup> This approach was used to prepare ethylene, propylene, mono and di-toluene, phenyl-propene derivatives, *para*-, *meta*-, and *ortho*-xylene, and 3,4-substituted thiophenes (Scheme 5b).<sup>39,40</sup> In particular, using xylene groups enables the synthesis of more sophisticated macrocycle alkoxythiophenes. Furthermore, Krompiec *et al.* extended the double Williamson etherification reaction to the synthesis of 3,4-phenylenedioxothiophene (PhEDOT) functionalized with electron-withdrawing groups *via* a double nucleophilic aromatic substitution of substituted benzenes in a one-pot reaction (Scheme 5c).<sup>41</sup>

### Proto decarboxylation

The final monomers are obtained through the double proto-decarboxylation of (5), commonly carried out until a decade ago, using Cu-based catalysts in quinoline as the solvent (Scheme 1).<sup>42</sup> Under these conditions, the complete conversion of electron-rich aromatic systems like 3,4-alkoxythiophenes is limited, leading to moderate yields. Besides, novel and environmentally friendly methodologies have been developed due to the toxicity of the reaction media and the time-consuming experimental procedure. For example, using different metal





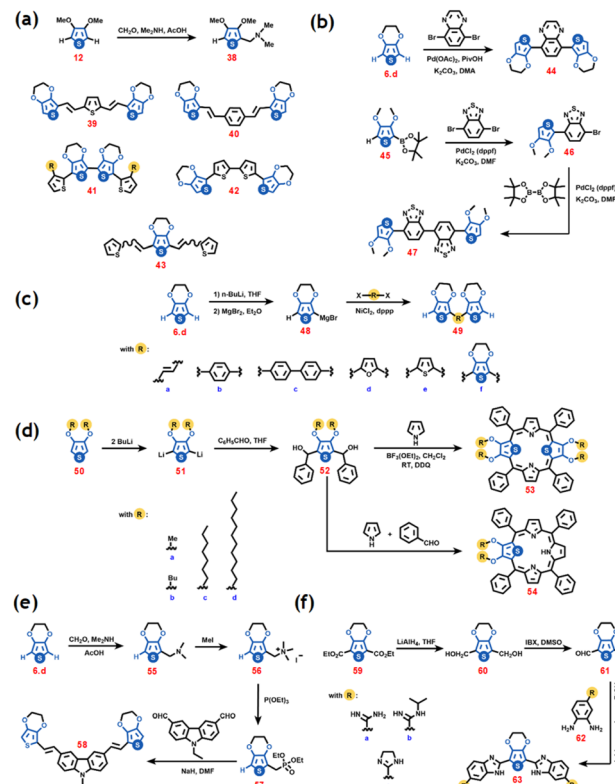
Scheme 6 Reactions of the double proto-decarboxylation of 3,4-alkoxythiophenes.

phthalocyanines (PC) of Cu, Zn, Co, Ni, Mn, Mg, Fe, and Ag as catalysts allows decarboxylation in aqueous media and at mild temperatures (Scheme 6).<sup>43</sup> Recently, Cisneros-Pérez *et al.* developed a highly efficient, low-temperature, and toxic-solvent-free proto-decarboxylation reaction with  $\text{Ag}_2\text{CO}_3$  as a catalyst and in a microwave reactor.<sup>44</sup> This synthetic method presents a considerable improvement in yield and time (from hours to minutes) compared with decarboxylation based on  $\text{Cu}_2\text{Cr}_2\text{O}_7$  (Scheme 6).

### Chemical modification of the 2 and 5 positions

Interestingly, it is possible to fine-tune the physicochemical properties of 3,4-alkoxythiophenes by introducing additional  $\pi$ -conjugated groups within the aromatic structure of the monomer. For example, the formation of a Mannich-type base at one  $\alpha$ -position of the thiophene ring allows the functionalization of positions 2 and 5 (Scheme 7a).<sup>45</sup> However, the most straightforward alternative is *via* a direct C–H arylation of EDOT, catalyzed by clay-supported Pd.<sup>46</sup> This approach has given access to multiple mono- and bis-arylated EDOT-based functional  $\pi$ -conjugated molecules.

With a similar philosophy, donor–acceptor–donor monomers have been designed either by using a  $\text{Pd}(\text{OAc})_2$ -catalyzed direct heteroarylation of EDOT or *via* a Suzuki–Miyaura coupling synthetic pathway (Scheme 7b);<sup>47</sup> recently, deep eutectic solvents have been employed for these couplings, thereby avoiding the use of toxic solvents.<sup>48</sup> In this context, different methodologies involving metallic catalysts have been developed. For example, the mono-arylation of Grignard-type EDOT catalyzed by  $\text{NiCl}_2$  in 1,3-bis(diphenylphosphine)-propane allows the introduction of conjugated structures, such as *para*-phenylene, vinylene, furane, or thiophene (Scheme 7c).<sup>49</sup> Furthermore, thioporphyrins were produced in a three-step synthetic pathway; at first, the reaction between the corresponding 3,4-diakoxothiophene and butyl-lithium to generate the organolithium compound, followed by a condensation with benzaldehyde, treated with boron trifluoride etherate, and finally the proper oxidation with 2,3-dichloro-5,6-dicyano-1,4-benzoquinone (Scheme 7d).<sup>50,51</sup> Nonetheless, generating a Mannich-type base at one  $\alpha$ -position of the thiophene ring is a practical approach to overcome the use of metallic catalysts.



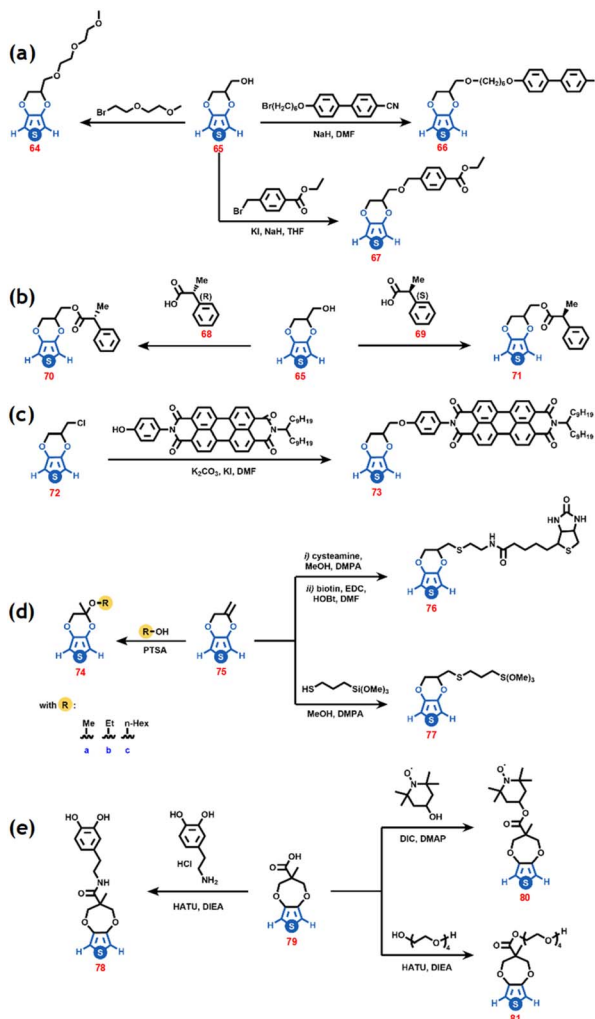
Scheme 7 Reactions employed for the functionalization of the positions 2 and 5 of the thiophene ring *via* (a) the formation of a Mannich type-base, (b) a  $\text{Pd}(\text{OAc})_2$  catalyzed direct heteroarylation, (c) a mono arylation of Grignard-type alkoxythiophenes and (d) the generation of organolithium thiophene. Schematic reactions for synthesizing (e) vinylene-linked *N*-ethyl-carbazole substituted thiophenes and (f) 2,5-substituted alkoxy thiophenes with benzimidazole rings.

Such an active group facilitates the efficient chemical coupling of *para*-phenylene–vinylene, thiophenylene–vinylene, substituted thiophene,<sup>52</sup> and vinylene-linked *N*-ethyl-carbazole<sup>53</sup> groups to the  $\alpha$ -position of thiophene (Scheme 7e). Stolić *et al.* developed a synthetic route based on the double oxidation of the ether moiety present in the 3,4-ethylenedioxothiophene-2,5-diethyl ether with  $\text{LiAlH}_4$  and IBX to the corresponding aldehyde, followed by the formation of the benzimidazole rings (Scheme 7f).<sup>54</sup>

### Ethylene and propylene bridge modification

In addition to the above-mentioned  $\alpha$ – $\alpha$  functionalization of the thiophene ring, it is possible to chemically modify the 3,4-ethylene or the 3,4-propylene groups. At first, through a Williamson etherification reaction, ethylene or propylene groups containing leaving groups, such as Cl and OH, are introduced to the monomeric unit.<sup>55</sup> Afterward, it is possible to substitute the halogen atoms to functionalize 3,4-alkoxythiophene. Different pendant groups have been introduced to the 3,4-alkoxy structure, ranging from polyethers<sup>56</sup> and long alkyl chains<sup>57</sup> to bulky groups such as 4-(6-bromohexyl-oxy)-40-cyano biphenyl ether<sup>58</sup> and perylenebisimide, hydroxymethyl- or chloromethyl-substituted EDOT (65 or 72) (Scheme 8a and 8b).<sup>59</sup> For





**Scheme 8** The alkoxy bridge modification using (a) hydroxymethyl-substituted EDOT (68), (b) ethylene or propylene group containing salient groups, (c) chloromethyl-substituted EDOT (72), (d) exomethylene-3,4-ethylenedioxythiophene (75) and (e) ProDOT carboxylic acid as starting building blocks.

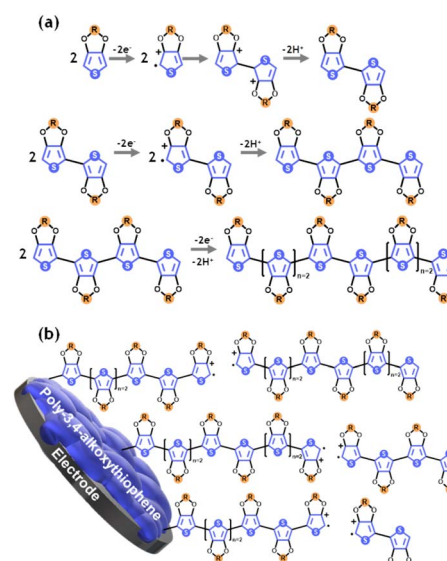
example, Dong *et al.* reported the successful anchoring of (R)- and (S)-2-phenyl propionic acid as pendant groups to Me-EDOT, where the obtained monomers retain the configuration of the initial chiral reactant (Scheme 8c).<sup>60</sup> The incorporation of crown ether into compound 72 produced CP with enhanced properties;<sup>61</sup> after several synthetic steps it is possible to attach malimide derivatives from the same starting compound to prepare human cell platforms.<sup>62</sup>

A helpful alternative is using exomethylene-3,4-ethylenedioxythiophene (emEDOT) (75) as a versatile building block. This can be obtained by the reaction between the mixture of EDOT-CH<sub>2</sub>OH and ProDOT with *para*-toluenesulphony chloride to obtain the tosylate ester, and after crystallization, EDOT-CH<sub>2</sub>OpTS can be separated, and this at last, in the presence of potassium tert-butoxide, generates emEDOT.<sup>63</sup> With this monomer as a starting unit, it is possible to functionalize the 3,4-ethylene group with many substituents (Scheme 8d). Finally, ProDOT carboxylic acid (ProDOT-COOH) (79) was synthesized

by *trans*-etherification of 1,3-diol and 3,4-dimethoxy-thiophene under acidic conditions. From this starting monomer, it is possible to substitute the OH from the carboxylic group *via* a classic esterification reaction with different redox active moieties, *i.e.*, dopamine, hydroxy-TEMPO, or tetra ethylene glycol (Scheme 8e).<sup>64</sup> The central sp<sup>3</sup> carbon of ProDOT has been symmetrically functionalized to attach diverse substituents, for example azide, triazole,<sup>65</sup> aliphatic alkyl ether chains,<sup>66</sup> alkyl ester chains,<sup>67</sup> glyme side chains,<sup>68,69</sup> and disulphide<sup>70</sup> among others. These monomers have shown excellent properties for use in technological applications.

## Chemical and electrochemical polymerization

As is well known,  $\pi$ -conjugated monomers are suitable starting units for generating conducting polymers. Commonly, this is achieved by following an oxidative radical polymerization mechanism, which involves the formation of highly reactive species, *i.e.*, radical anions or dications. In this context, the oxidative dimerization and oligomerization pathway is the most studied polymerization mechanism in conducting polymers (Scheme 9a). At first, oxidation of the monomer takes place to form the corresponding radical cation, which dimerizes at the  $\alpha$ -position of the conjugated ring, with the subsequent deprotonation step to recover aromaticity. Afterwards, the formed dimers undergo a series of consecutive oxidation and coupling-deprotonation steps, continuously increasing the oligomers' length. However, the coupling pathway followed by the formed oligomeric radical cations strongly depends on the substituents and their molecular position within the monomer. For example, for the simple thiophene,  $\alpha$ - $\alpha$ -,  $\alpha$ - $\beta$  and  $\beta$ - $\beta$ - oligomeric couplings can take place, leading to the formation of highly



**Scheme 9** (a) Oxidative dimerization and oligomerization mechanism of 3,4-alkoxy thiophenes and (b) long chain propagation catalyzed by solid-state redox processes.

cross-linked films. Thus, as stated above, the electron-donating effect of the 3,4-alkoxy groups favours  $\alpha$ - $\alpha$ -couplings, producing well-defined oligomeric structures. Since the polymerization conditions can fine-tune the electrical, electrochemical, mechanical, and optical properties of such materials, this section summarizes the recent advances in the chemical and electrochemical polymerization of 3,4-alkoxythiophenes and the possible post-functionalization of the obtained conjugated films. The reader can consult the reviews and books in this field for more details concerning the different oxidative and reductive polymerization mechanisms.<sup>4,8,71</sup>

### Homogeneous redox polymerization

The homogeneous oxidative redox polymerization takes advantage of the thermodynamically favored reduction of a redox initiator, *i.e.*,  $\text{FeCl}_3$ .<sup>72</sup> Thus, in the previously mentioned mechanism, the oxidant dissociates into active species before the oligomerization reaction.<sup>73</sup> Such highly reactive oxidants cause the continuous generation of the radical cation of the monomer and its subsequent oligomers, which, *via* the oxidative dimerization pathway, produce the corresponding CP. Among all the different  $\pi$ -conjugated systems, PEDOT produced with homogeneous redox polymerization is one of the few conducting polymers that have become an industrial reality.<sup>74</sup> However, solutions of doped monomers and oligomers are highly unstable due to their different thermodynamic standard redox potentials. An interesting alternative to slowing down the oxidative process is to increase the pH slightly during homogeneous redox polymerization. Different approaches have been developed to produce highly conducting PEDOT films, ranging from the use of vapour phase polymerization (VPP)<sup>75</sup> and high temperature-non-hydrolyzed oxidants ( $\text{Fe}_2(\text{SO}_4)_3$ ),<sup>76</sup> to ultrasonic spray polymerization (USPo) (producing nanospheres of PEDOT)<sup>77</sup> and organic solid Brønsted acids (*p*-toluenesulfonic acid), to generate  $\alpha$ - $\alpha$  carbon bonds.<sup>78</sup> The use of mechanochemistry with 3,4-alkoxythiophenes,  $\text{Fe}^{3+}$  salts as an oxidant and  $\text{NaCl}$  as an additive, allows the solvent-free synthesis of the corresponding polymers.<sup>79,80</sup> Also, considerable efforts have been made to achieve homogeneous redox polymerization of alternative 3,4-alkoxythiophenes. For example, a family of soluble donor-acceptor ProDOT-based films has been reported. Such conjugated polymers were synthesized through a Knoevenagel polycondensation or a Yamamoto coupling polymerization.<sup>81</sup> The solid-state polymerization of 3,4-ethylenedioxythiophene-methanol (EDTM) derivatives was carried out from the 2,5-dihalogenated monomers, which induces the solid-state radical polymerization at slightly higher temperatures (80 °C for 24 h),<sup>82</sup> which is an alternative to  $\text{Br}_2$  oxidative polymerization using the same starting materials.<sup>83</sup> Lu *et al.*, designed 3,4-dialkoxythiophene-based copolymers using a palladium-catalyzed direct C-H arylation polymerization (DHAP). Such a methodology produces the linked dithiazole unit with the alkyl-substituted 3,4-dialkoxythiophene derivatives.<sup>84</sup> Following this approach, copolymers of ProDOT and acyclic dioxythiophene (AcDOT) with PhEDOT were designed to increase the chemical stability of the

starting monomers.<sup>85</sup> Water-processable polythiophenes with conductivities up to 1000  $\text{Scm}^{-1}$  useful for roll-to-roll processing were obtained in this way.<sup>86</sup> An alternative for these Pd-based hetero couplings employing the indophenine reaction to incorporate an aromatic connector between thiophene moieties is gaining interest.<sup>87-89</sup>

Furthermore, the homogeneous redox polymerization approach has been successfully coupled with templated substrates to generate sophisticated nanostructured conducting films. Such highly ordered surfaces present an increasing potentiality in microelectronics and photonic devices for energy storage and biological applications. For example,  $\text{V}_2\text{O}_5$  nanofibers were used as sacrificial templates during the chemical synthesis of PEDOT nanofibers.<sup>90</sup> Monodimensional (1-D) nanostructured PEDOT systems (tubes, thimbles, rods, and belts) were obtained *via* oxidative polymerization using  $\text{Al}_2\text{O}_3$  membranes as a template.<sup>91</sup> With the same philosophy, PEDOT: VDOT thin films were obtained by chemical oxidation using a sol-gel generated surface of di-Si(OEt)<sub>3</sub> functionalized with a free radical initiator (AIBN), which acts as an anchor point for EDOT oligomerization.<sup>92</sup> In addition to EDOT, the homogeneous redox polymerization of ProDOT-based monomers has been successfully carried out. In principle, these materials were used as model systems for optoelectronic applications; they have recently gained considerable interest in the study of solid-state electrochemical doping.<sup>68,93</sup> Although homogeneous redox polymerization is so far the classic method for producing poly-3,4-alkoxythiophene-based devices, the main limitation is the poor control of the doping level within the oligomeric units, due to the high thermodynamic redox potential value of the required oxidants and the impurities that are frequently found in the polymer matrix. In this context, electrochemical polymerization is a powerful tool for overcoming and controlling the properties of the prepared materials.

### Electrochemical polymerization

As stated above, electropolymerization offers several advantages over homogeneous polymerization, including morphology control and efficient fine-tuning of the doping level. This is commonly performed using a conventional three-electrode system composed of a working, counter, and reference electrode. In such a setup, the anodic reactions are triggered by controlling the thermodynamic (potentiodynamic or potentiostatic methods) or kinetic (galvanostatic method) parameters associated with the oxidation of the monomers. Thus, the oxidative dimerization pathway occurs at the electrode/electrolyte interface, followed by an electrostatic deposit of short-chain oligomers (nucleation).<sup>94</sup> Afterwards, three-dimensional growth catalyzed by solid-state redox processes takes place. In addition, electrochemical methods can produce templated electrodes to design sophisticated and highly structured materials (Scheme 9b).<sup>95</sup> Interestingly, the properties of the resulting polymers depend on the electrochemical technique used.<sup>96</sup>

Once again, electropolymerization of EDOT is the most studied system since the produced polymer exhibits high



electrochemical stability during multiple charge/discharge cycles.<sup>97</sup> Furthermore, heterogeneous redox polymerization can be carried out in the presence of different doping ions, to fine-tune the electrochemical properties.<sup>98</sup> Due to its efficient electropolymerization, EDOT has been used as a building block to design multiple functionalized conducting polymers. PEDOT films functionalized with cyanobiphenyl derivatives,<sup>99</sup> sodium sulfinopropyl,<sup>100</sup> electron acceptor groups such as perylenebisimide,<sup>59</sup> 9,10-anthroquinone (AQ), perylenetetracarboxylic diimide (PTCDI), and 11,11,12,12-tetracyano-9,10-anthraquinodimethane (TCAQ)<sup>101</sup> or biocompatible groups, *i.e.*, biotin<sup>102</sup> have been designed, among many others. An exciting alternative to facilitate the electropolymerization and minimize steric hindrance is to use dimeric and trimeric units as starting compounds.<sup>103–106</sup> For example, the dimer and trimer of Phe-DOT present a higher reactivity than the monomer unit, which facilitates electropolymerization.<sup>107</sup> Besides, starting from more conjugated monomers decreases the oxidation potential; thus, the redox properties of the CPs are enhanced. A classic example is thiophene, where bithiophene is always preferred to obtain PTh CPs due to the thiophene paradox.<sup>71</sup> EDOT-aldehyde-bearing thiophene-EDOT units facilitate the incorporation of functional groups on the oligomeric backbone.<sup>108</sup> Another alternative is the design of  $\pi$ -conjugated 3D systems, where EDOT groups are located strategically on the  $\alpha$  and  $\beta$  positions of bithiophene to generate a 3D template unit (Fig. 1a).<sup>109</sup> In addition, the electrochemical co-polymerization of EDOT with alternative conjugated groups has gained considerable attention.<sup>110</sup> For example, bithiophene-*alt*-thiophene-*S,S*-dioxide generated by anodic coupling of 2,5-bis(2-thienyl)thiophene-*S,S*-dioxide substituted with EDOT exhibits peculiar magnetic and luminescent properties.<sup>111</sup> The efficient coupling of EDOT electrochemically linked to thienopyrazine, cyclopentadithiophen-4-one or 4-dicyanomethylenecyclopentadithiophene produces low-gap thiophene-based materials.<sup>112</sup> Electrochemical co-polymerization of ferrocene-derived EDOT with hydroxymethyl-EDOT and oligo(oxyethylene)di-EDOT leads to chemically and electrochemically stable polymeric films.<sup>113</sup> In particular, the non-covalent intramolecular S–O interactions of EDOT promote planar conformations of the  $\pi$ -conjugated systems during electrochemical copolymerization. For example, sulphur–bromine interactions lead to a strengthened and rigid backbone in a co-polymer formed by EDOT and 3-bromothiophene.<sup>114</sup> However, multiple efforts have been made to polymerize alternative 3,4-alkoxythiophene systems electrochemically. For example, electropolymerized derivatives of PhDOT modified with naphthylmethyl-, 1-naphthylmethyl-, and 9-anthracenylmethyl-groups, exhibit nanostructured surfaces, providing these materials with unconventional physicochemical properties (Fig. 1b).<sup>32</sup>

Recently, the electropolymerization of 3,4-*ortho*-xylendioxathiophene (XDOT) in organic media was carried out.<sup>115,116</sup> Such a polymer exhibits a potentiodynamic mirror image associated with fast electron transfer, attributed to an *in situ* internal oligomeric order caused by the presence of a xylene unit. This polymeric internal arrangement leads to an improved insulating/conducting transition of PXDOT compared to

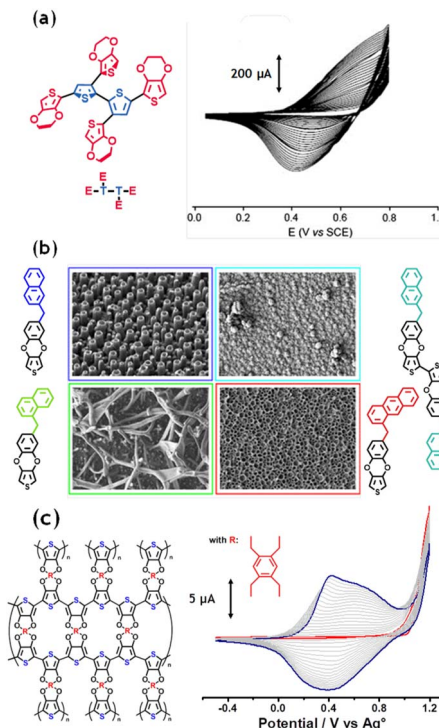


Fig. 1 (a) Chemical structure of a 3D template formed by four EDOT groups attached at the  $\alpha$  and  $\beta$  positions of a bithiophene structure (left) and potentiodynamic electropolymerization of the corresponding 3D oligomeric material obtained in 10 mM monomer 0.10 M  $\text{Bu}_4\text{NPF}_6$ /ACN solution. Reproduced from ref. 109 with permission from Elsevier, copyright 2008. (b) Chemical structure and SEM images of the top view of electrodeposited functionalized PhDOT modified with naphthylmethyl-, 1-naphthylmethyl-, and 9-anthracenylmethyl-groups. Reproduced from ref. 32 with permission from the American Chemical Society, copyright 2019. (c) Chemical structure of ordered 3D oligomeric networks formed by PDbDOT and electrochemical polymerization of DbDOT obtained in a 5 mM monomer 0.1 M  $\text{TBAPF}_6$ /CH<sub>2</sub>Cl<sub>2</sub> solution. Reproduced from ref. 118 with permission from Elsevier, copyright 2025.

PEDOT or bithiophene.<sup>117</sup> Furthermore, it has been proposed that during the electropolymerization of 3,4-duren-bidioxathiophene (DbDOT) ordered 3D oligomeric networks could be generated (Fig. 1c).<sup>118</sup> This is associated with the double thiophene core within the monomeric unit and the spatial conformation provided by the duren moiety. Poly-ProDOT derivatives containing different functional groups such as oxyphenyl methanol ( $-\text{OPhCH}_2\text{OH}$ ), oxybenzyl ( $-\text{OBz}$ ), bromide ( $-\text{Br}$ ), and tosyl ( $-\text{OTs}$ ) have been synthesized and electropolymerized.<sup>119</sup> A direct correlation was observed between the oxidation potential of the monomer and the electron-donating or electron-withdrawing character of the substituent at the ether bridge. The presence of these substituents leads to a more pronounced  $\pi$ – $\pi$  intermolecular stacking, improving the charge transport.

Although electrodeposition of 3,4-alkoxythiophenes is carried out in non-aqueous media, mainly due to the monomer's low solubility in water, the possible formation of micellar structures employing a surfactant, *i.e.*, sodium dodecyl sulfate



(SDS) or Triton X-100, allows the electrochemical polymerization of EDOT in aqueous media.<sup>120,121</sup> This approach has been extended to alternative 3,4-alkoxythiophene monomers such as hydroxyl-methylated-EDOT<sup>55</sup> or 3,4-dimethoxythiophene.<sup>122</sup> However, the functionalization of EDOT facilitates electro-polymerization in aqueous media. For example, introducing hydroxymethyl groups significantly improved the polymerization and electroactivity of the polymer generated in aqueous media.<sup>123</sup> Additionally, Sun *et al.* carried out the polymerization of 2'-aminomethyl-3,4-ethylenedioxythiophene hydrochloride (EDOT-MeNH<sub>2</sub> HCl) in an aqueous solution, obtaining highly stable polymers with efficient electrochromic properties.<sup>124</sup>

In addition to organic and aqueous media, multiple efforts have been carried out to explore the possible electro-polymerization in alternative and, so far, unconventional solvents, such as ionic liquids or liquid crystals. For example, the oxidative electropolymerization of EDOT in an aqueous solution of hydroxypropyl cellulose (HPC) acting as an inert chiral nematic liquid crystal medium led to the generation of chiral PEDOT with good electrochemical stability and reversible optoelectronic properties.<sup>125</sup> With a similar philosophy, Matsushita *et al.* used a chiral nematic liquid crystal system to electrochemically polymerize EDOT and bis-EDOT on helical carbon and graphite films.<sup>126</sup> Furthermore, it has been demonstrated that the use of deep eutectic solvents such as choline chloride-urea (reline) and choline chloride-ethylene glycol (ethaline) leads to changes in the morphology and electrochemical properties of PEDOT,<sup>127,128</sup> which enable the possible use of these surfaces for sensing applications.

Finally, post-polymerization functionalization allows fine-tuning of the chemical, electrochemical, electrical, and optical properties of CPs. For example, poly-3-(*x*-haloalkyl) thiophenes were post-functionalized with tetrathiafulvalene (TTF) derivatives to improve their electrochemical properties. These materials exhibit a lower insulating/conducting transition onset potential and an improved ionic permeability compared with PEDOT.<sup>129</sup> With a similar philosophy, Wei *et al.* used thiol-ene “click” chemistry to covalently attach alkyl-thiols to electrochemically deposited poly-(ProDOT-diene). The presence of such pendant groups modifies the surface chemistry of the CP, which is reflected in changes in its physico-chemical properties, *i.e.*, capacitance or hydrophilicity.<sup>130</sup> Electrochemically driven post-functionalization of a poly succinimidyl ester EDOT derivative and oligo(oxyethylene)diEDOT with ferrocene-labelled oligonucleotides (Fc-ODNs) has been carried out for the design of bioelectrochemical sensors.<sup>131</sup> In another example, co-polymers of dihexyl-substituted EDOT (Hex<sub>2</sub>-EDOT) and azidomethyl-EDOT (N<sub>3</sub>-EDOT) have been electrochemically functionalized with an electron-accepting phthalimide substituent by “click chemistry”.<sup>132</sup>

## Property control by physicochemical interactions

For decades, diverse effects of the 3,4-alkoxythiophenes have been recognized as an important issue to consider during

polymer engineering, particularly in the case of conducting or semiconducting organic polymers. For example, the band gap of these materials depends on five energy contributions: the energy related to the degree of bond length alternation, the mean deviation from planarity, the aromatic resonance energy of the cycle, the inductive or mesomeric electronic effects of substitution, and the intermolecular or interchain coupling in the solid state.<sup>133</sup> Recently, an excellent review addressing this last contribution has reminded us that this sometimes unattended aspect is important to consider for solid-state applications in these organic conductors.<sup>134</sup> One of the most important interactions in the polymer chain is  $\pi$ - $\pi$  stacking, which depends on the ability to form long-range planar structures. Here, non-covalent intra-chain interactions, which generate conformational locks of the polymer backbone, favour planar structures between adjacent monomers. For poly 3,4-alkoxythiophenes, noncovalent O $\cdots$ S interactions are present to control the planarity, whereas when nitrogenated hetero copolymers are used, N $\cdots$ S interactions guide the planarity of the material (Fig. 2).<sup>135</sup>

On the other hand, side-chain interactions of the polymers contribute to controlling the material's properties. For example, the presence of glycolated chains favours the processability of the poly-3,4-alkoxythiophenes in aqueous media with good electronic properties.<sup>86</sup> In this example, a combination of O···S interactions of the central heterocyclic moiety with the polar chains was an innovative proposal to produce large CP surfaces. Large alkyl chains on the 3,4-alkoxythiophenes promote van der Waals interactions, which generate a large range order in the polymer. Examples can be found in those used for organic electrochemical transistors,<sup>136</sup> a similar situation to that observed with 3-hexylthiophene used for organic solar cells.<sup>137</sup> Electronic properties like conductivity, charge mobility, band gap, and optoelectronic properties, among many others, depend on these intra- and inter-chain interactions. Therefore, the hydrophilicity and hydrophobicity of the chains<sup>138</sup> and their chemical structure (linear or branched)<sup>69,139</sup> modulate the

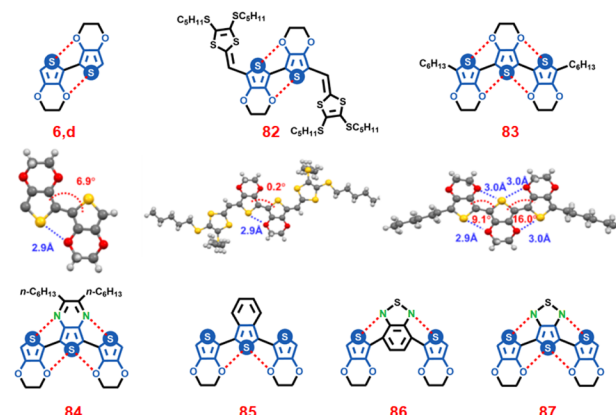


**Fig. 2** Chemical and single-crystal structures of 3,4-alkoxythiophenes showing the O···S interactions in homo polymers and N···S interactions in heterocopolymers. Adapted from ref. 135 with permission from the American Chemical Society, copyright 2017.



Table 2 Conductivity, anodic window, maximal absorption, and reported applications of representative poly-3,4-dialkoxythiophenes

Monomer	Polymer conductivity ( $\text{S cm}^{-1}$ )	Polymer anodic window	Absorption maxima	Applications	Reference
PEDOT (6 <i>a</i> ) PEDOT:PSS	$10^{-4}$ to $10^3$	-0.6 V to 0.3 V vs. Ag/AgCl	600 nm	Solar cells, supercapacitors, transparent conductive electrodes, sensors, and drug delivery	76, 115 and 275
PXDOT (6 <i>m</i> )	100 mS (Conductance)	-0.3 V to 0.6 V vs. Ag/AgCl		Electroanalysis	116
DxDOT (Fig. 1c)	9 mS (Conductance)	-0.25 V to 0.5 V vs. Fe/Fe <sup>+</sup>	420 nm	3-D nanostructured surfaces	118
ProDOT-OBn <sub>2</sub> (16)		-0.1 V to -0.3 V vs. SCE	578 nm, 632 nm	Electrochromism	31
PhEDOTS (17 <i>a</i> – <i>c</i> )		0.7 V to 1.1 V SCE		Hydrophobic nanostructured surfaces	32
Stereo- and regioregular PEDOTS (18 <i>a</i> – <i>j</i> )		-1.0 V to -0.5 V vs. Fe/Fe <sup>+</sup>		Enantioselective electroanalysis	30
Poly(spiroBiPpDOT) (19)		-0.45 V to 0.85 V vs. Fe/Fe <sup>+</sup>	486 nm	Electrochromism and solar cells	34
Poly(2,2',3,3'-tetrahydro-2,2'-bithiopheno[3,4- <i>b</i> ][1,4]dioxine) (20)		0.0 V to 1.0 V vs. Ag/AgCl	481 nm	Electrochromism	35
( <i>E</i> )-1,2-bis[2-(3,4-ethylenedioxy) thiényl] vinylene (49 <i>a</i> )	20	-0.6 V to 0.4 V vs. Ag/Ag <sup>+</sup>	590 nm	Electrochromism	49
( <i>E</i> )-1,2-bis[2-(3,4-ethylenedioxy)thiényl] benzene (49 <i>b</i> )	2.0	-0.2 V to 0.2 V vs. Ag/Ag <sup>+</sup>	495 nm	Electrochromism	49
2,2':5',2''-ter(3,4-ethylenedioxy) thiophene (49)	10	-1.2 V to 0.9 V vs. Ag/Ag <sup>+</sup>	442 nm	Electrochromism	49
Hydroxymethylene-3,4-ethylenedioxythiophene (65)	18 to 65	-0.6 V to 0.6 V vs. Ag/AgCl	520 nm	Electroanalysis	55
4-(6 oxymethylenedioxythiophene hexyloxy)-4'-cyanobiphenyl (66)	0.03	-0.6 V to 0.6 V vs. Ag/Ag <sup>+</sup>	600 nm to 660 nm	Electrochromism	58
(2,3-dihydrothieno[3,4- <i>b</i> ][1,4]dioxin-2-yl methyl 2-phenylpropanoate)(70 and 71)		-0.4 V to 0.5 V vs. Ag/AgCl	627 nm	Electroanalysis	60
Perylenetetracarboxylic-bisdiimide-EDOT (73)		-0.5 V to 0.75 V vs. Fe/Fe <sup>+</sup>	400 nm to 850 nm	Organic solar cells	59
emEDOT (74)		0.1 V to 0.8 V vs. Fe/Fe <sup>+</sup>		Building block for CPs	63

electronic properties. In addition to these, the doping level is a crucial parameter to consider. The magnitude of this parameter directly impacts the electrical, electrochemical, and optoelectronic response of the material. Commonly this can be fine-tuned by using the nature of the dopant (counter-ion), the side-chain structure, the polymerization method and post-polymerization treatments.<sup>4,8,140,141</sup> More detailed information about the relationship between the polymer structure and properties can be found in specialized literature dealing with organic semiconductors or polymer engineering.<sup>142,143</sup> Nonetheless, it is evident that the nature of the 3,4-alkoxy group controls the physicochemical properties of the polymer, thus guiding the selection of the possible application (Table 2).

## Applications of poly-3,4-alkoxythiophenes

Due to their outstanding physicochemical properties, poly-3,4-alkoxythiophenes have gained considerable attention in multiple applications. Most of these utilize the polymers' conductivity, their inherently large electroactive area, reversible insulating/conducting transition, or efficient color switching. It is essential to highlight that most reported systems use PEDOT-based polymers.<sup>144</sup> A representative group of these materials is shown in Table 2, where it can be observed that properties such as conductivity, polymer anodic window, and UV maxima absorption can be manipulated to convenience with the modification of the lateral chains of the thiophenic core. The conductivity of the CP can be enhanced by generating hydroxyl

moieties on the polymer surface through post-processing side chain removal, resulting in quasi-metal-like electron transport with conductivities of *ca.* 1200 S cm<sup>-1</sup>,<sup>68,145</sup> thereby reviving its use. Thus, recently, novel and unexplored poly-3,4-alkoxythiophenes have begun to replace these well-known materials. This section describes the various applications of poly-3,4-dialkoxythiophenes over the past few years.

### Batteries and supercapacitors

Due to their relatively fast charge/discharge transition, conducting polymers, particularly 3,4-alkoxythiophenes, have become a promising alternative for the design of energy storage devices.<sup>146-149</sup> For example, poly-(8-bis(2,3-dihydrothieno[3,4-*b*][1,4]dioxin-5-yl)-3,3-dimethyl-3,4-dihydro-2*H*-thieno[3,4-*b*][1,4]dioxepine), exhibits a 3D porous network, which significantly enhances the capacitance performance of the material.<sup>150</sup> However, problems concerning the ionic transport within the polymer matrix and mechanical and electrical stability hinder the use of such conjugated materials. Therefore, the possible use of conducting polymers as redox-active materials for high-capacity commercial devices remains challenging. Research in this field has focused on developing composites formed by a conducting matrix and alkoxythiophenes.<sup>151-154</sup> Recently, the efficient conductivity of poly-3,4-alkoxythiophenes has become a promising alternative as anodic and cathodic binders to enable charge transfer through the electrode.<sup>155</sup> For example, dihexyl-substituted poly-ProDOT (PProDOT-Hx<sub>2</sub>) was used as a cathodic binder, showing a five-fold increase in capacitance at high discharge rates compared to the classic insulating

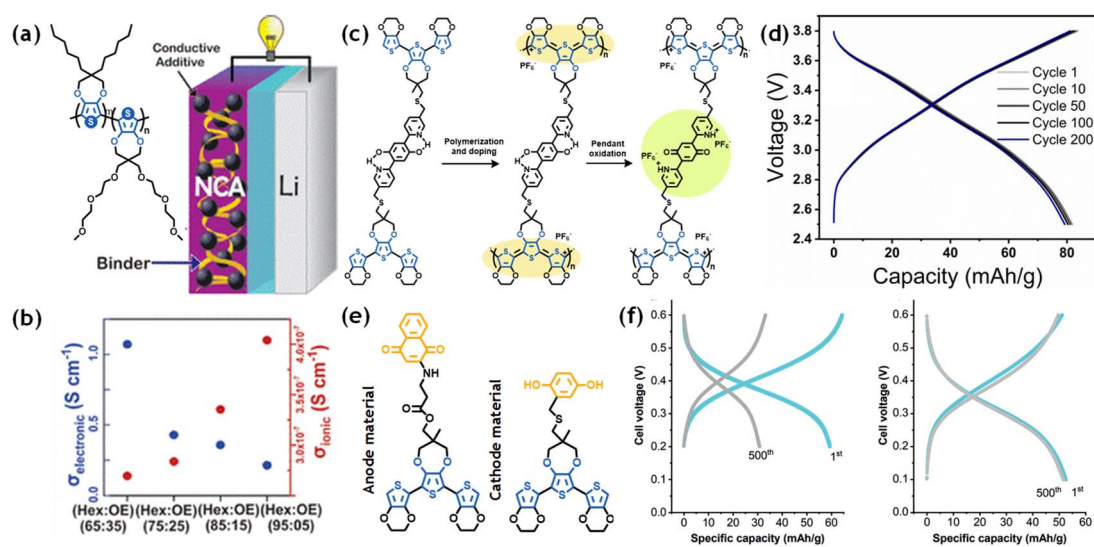


Fig. 3 (a) Chemical structure of the copolymer of PProDOT-Hx<sub>2</sub> and oligoether-substituted poly-ProDOT with possible use as a conductive cathode binder in lithium-ion batteries. (b) Electronic (left blue axis) and ionic (right red axis) conductivities of the copolymer series. Adapted from ref. 157 with permission from the American Chemical Society, copyright 2022. (c) Schematic illustration of the EDOT-ProDOT-EDOT trimer functionalized with a combined hydroquinone-trap pendant, with a representation of electropolymerization and the redox active group. (d) Voltage profile for galvanostatic charge and discharge for multiple cycles (indicated in the figure) of the proton acceptor poly-3,4-alkoxythiophene acting as the organic cathode. Adapted from ref. 165 with permission from the Royal Chemical Society, copyright 2020. (e) Chemical structures of the EDOT-ProDOT-EDOT trimers functionalized with NQ/NQH<sub>2</sub> and Q/QH<sub>2</sub> acting as anodic and cathodic redox groups, respectively. (f) Voltage profile for the first (cyan) and the 500th cycle (grey) of a battery working at room temperature (left plot) and 24 °C (right plot). Adapted from ref. 166 with permission from John Wiley and Sons, copyright 2020.



polyvinylidene fluoride.<sup>156</sup> Such an enhancement in the performance of the cathode is associated with an open polymeric structure and increased solvation of the PProDOT-Hx<sub>2</sub> chains, which improve the ionic conductivity. Furthermore, Thompson *et al.* demonstrated that using copolymers of PProDOT-Hx<sub>2</sub> and oligoether-substituted poly-ProDOT makes it possible to fine-tune the ionic conductivity of the binder (Fig. 3a and b).<sup>157</sup> An interesting alternative is using conducting polymers as redox-active materials and conducting electrodes. Such an approach has gained considerable attention in the design of all-organic batteries. For this, the 3,4-alkoxythiophene monomers are functionalized with a redox-active group, *i.e.*, TEMPO or quinone-type moieties.<sup>158–163</sup> In addition, by functionalizing the pendant quinone groups with electron-withdrawing substituents, an increase in the formal redox potential of the redox-active moiety has been observed. The synergy between the conductive properties of PEDOT and these active pendant groups makes these polymers a promising alternative for the design of high-voltage cathode materials for lithium-ion batteries.<sup>164</sup> With a similar philosophy, a poly-3,4-alkoxythiophene cathode material, functionalized with a hydroquinone group as a redox group and pyridine moieties acting as proton acceptors, was designed (Fig. 3c).<sup>165</sup> For this, a trimer formed by EDOT and ProDOT units was used as a conducting material, exhibiting highly reversible redox properties. When using this polymer as an organic cathode coupled to a lithium foil anode, efficient cycling with a high-capacity retention of 99% after 100 cycles and 98% after 200 cycles was achieved (Fig. 3d). Finally, an all-organic redox-polymer-based proton battery was designed.<sup>166</sup> In this case, the EDOT-ProDOT-EDOT trimers were used as conducting materials. In contrast, the benzoquinone/hydroquinone (Q/QH<sub>2</sub>) and naphthoquinone/naphthohydroquinone (NQ/NQH<sub>2</sub>) systems act as cathodic and anodic redox groups, respectively (Fig. 3e). Such an organic battery exhibits good stability (around 85% after 500 cycles) and fast full-capacity charging (100 seconds) at low working temperatures (−24 °C) (Fig. 3f). Recently, a quinizarin-poly-3,4-alkoxythiophene was used as the cathode in an all-organic proton battery.<sup>167</sup> Once again, in combination with NQ/NQH<sub>2</sub>-poly-3,4-alkoxythiophene, acting as anode, a good cycling stability of the battery (80% after 500 cycles) was obtained. With a similar philosophy, donor-node-acceptor ambipolar 3,4-alkoxythiophenes have been used for the design of wide-voltage and high-stability super capacitors.<sup>168,169</sup> For this, EDOT and phthalic anhydride derivatives act as donor and acceptor units, respectively, whereas the linker moiety works as a separator, producing independent redox activity of the electroactive groups. The simultaneous p- or n-doping within the polymer increased the operating voltage of supercapacitors composed by this material.

### Electrochromism

Optical transitions of  $\pi$ -conjugated polymers have gained considerable attention in electrochromic devices due to the possible generation of different optical absorption bands during the charging/discharging process. Such outstanding

features of these materials enable the possible fine-tuning of the film coloration by controlling the applied potential. Among the different 3,4-alkoxy thiophenes, PEDOT is an electrochromic material due to its efficient optical transition between dark blue and slightly transparent.<sup>170,171</sup> In its discharged state, PEDOT presents an optical absorption between 1.5 eV and 2 eV (dark blue), whereas, in its conducting state, the maximum absorption is at 0.6 eV (transparent in the visible region). However, different approaches have been used to improve the optical transition, extend the range of coloration, and improve the switching time. For example, by fine-tuning the chemical structure of the 3,4-alkoxy moiety, it is possible to improve the electrochromic properties of these materials. Reynolds's group studied the influence of linear and branched side chains on the optoelectronic properties of poly-3,4-alkylenedioxothiophenes.<sup>172</sup> Changing the side chain structure can modify the color, switching time, electrochromic contrast, and switching stability. ProDOT-based polymers with oligoether or mono and di-substituted amide functional groups have been designed by a similar approach.<sup>172,173</sup> Recently, Cumuru *et al.*, designed multichromic metallopolymers of PEDOT and poly-ProDOT by functionalizing the ethylene group with bipyridine-based Ru(II) complexes.<sup>174,175</sup> In this case, the wide range of color is attributed to the optical transition of the 3,4-alkoxythiophenes and the redox transitions of the metallic complexes.

An alternative approach is to design donor–acceptor monomers by functionalizing the EDOT moiety in the  $\alpha$ -position to combine the electrochromic properties of each conjugated unit. For example, different EDOT-*para*-phenylene-based polymers present a broad range of coloration, between red and blue, with fast transition times (0.9 s) and high coloration efficiency (305 C<sup>−1</sup> cm<sup>2</sup>) (Fig. 4a and b).<sup>176</sup> Liu *et al.* designed donor–acceptor EDOT-quinoxaline derivatives, which exhibit an optical transition between blue and transparent after electropolymerization.<sup>177</sup> Furthermore, with such systems, fast transition times ( $\approx$  0.5 s), high optical contrast (>50%), and coloration efficiency (427 C<sup>−1</sup> cm<sup>2</sup>) were obtained. Finally, considerable efforts have been made to extend the range of coloration of different  $\pi$ -conjugated monomers by producing copolymers with EDOT. Wang *et al.* used direct (hetero)arylation polymerization to obtain 2,7- and 3,6- substituted carbazole-EDOT copolymers.<sup>178</sup> The obtained materials present short response times (<1 s), high coloration efficiency (>370 C<sup>−1</sup> cm<sup>2</sup>), and a range of coloration between yellow and dark blue. Thiophene-benzothiadiazole-EDOT copolymers, obtained by electropolymerization, exhibit good transition times (<1 s) during multiple double pulse potentiostatic cycling, however, with relatively low coloration efficiency (<100 C<sup>−1</sup> cm<sup>2</sup>).<sup>179</sup> A copolymer based on EDOT-benzothiadiazole and ProDOT was designed using a similar approach.<sup>180</sup> The obtained polymer exhibited adsorption in almost the entire visible region in its neutral state and exhibited an enhanced optical contrast (>40%) compared with pristine ProDOT. Cyan, magenta and yellow colours were achieved by combining the electrochromic properties of ProDOT-based polymers with benzothiadiazole or *N*-octylcarbazole.<sup>181</sup> The trichromatic electrochromic device reproduces the entire color spectrum of the visible region by



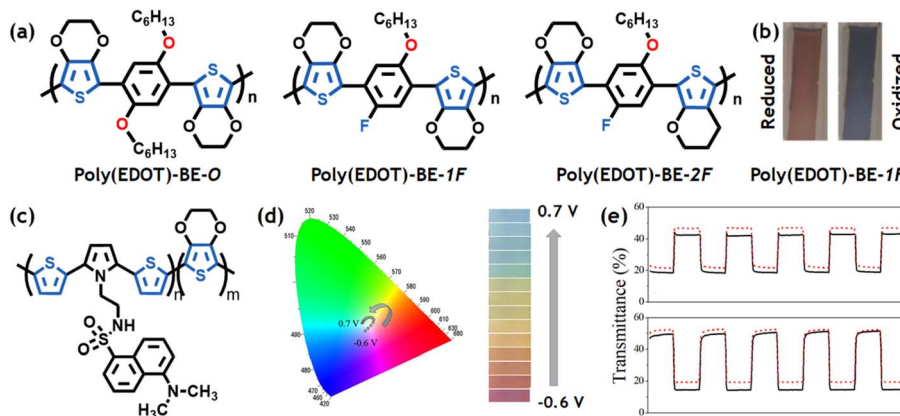


Fig. 4 (a) Chemical structures of different EDOT-*para*-phenylene-based polymers: poly(EDOT-BE-O), poly(EDOT-BE-1F), and poly(EDOT-BE-2F). (b) Optical pictures of the charged and discharged state of poly(EDOT-BE-1F). Adapted from ref. 176 with permission from Elsevier, copyright 2022. (c) Chemical structure of a copolymer formed by an *N*-dansyl substituted SNS derivative and EDOT. (d) Calculated color trajectory in the CIE 1931 color space (left) and optical images of the rainbow-like multi-electrochromic behavior of the copolymer at different oxidation potentials (indicated in the figure) (right). (e) Transmittance transients at  $\lambda = 560$  nm (top) and 990 nm (bottom) obtained during redox cycling. Adapted from ref. 190 with permission from Elsevier, copyright 2020.

fine-tuning the applied potential. Moreover, a low-power flexible electrochromic device was designed by immobilizing a copolymer formed by a branched 3,4-dialkoxy thiophene and a pyrene-substituted EDOT on multi-walled carbon nanotubes.<sup>182</sup> This system exhibits short transition times (below 3 seconds) and long cyclability (above 15 k cycles).

Recently, coupling the outstanding electrochromic properties of 2,5-dithienyl-*N*-substituted-pyrrole (SNS) and EDOT has gained considerable attention. Poly-SNS derivatives present well-defined redox processes, low switching times, and a broad range of coloration.<sup>183,184</sup> In particular, *N*-substituted SNS-EDOT copolymers exhibit multi-electrochromic behaviors with fast switching times and good coloration efficiencies.<sup>185–188</sup> For example, poly(EDOT-*co*-1-(3,5-bis(trifluoromethyl)phenyl)-2,5-di(thiophen-2-yl)-1H-pyrrole) presents an optical contrast of 41% with a coloration efficiency of  $258 \text{ C}^{-1} \text{ cm}^2$  and 1.4 s transition time.<sup>189</sup> Ribeiro *et al.* recently obtained a rainbow-like multi-electrochromic copolymer by coupling an *N*-dansyl substituted SNS derivative and EDOT (Fig. 4c and d).<sup>190</sup> This polymer presents a multi-chromatic contrast at 560 and 990 nm of 25 and 35, respectively, with a coloration efficiency between 110 and  $180 \text{ C}^{-1} \text{ cm}^2$  and fast switching time (<1.0 s) during redox cycling (Fig. 4e). Nicolini *et al.* demonstrated that the inclusion of EDOT improves the kinetics of electropolymerization of an *N*-aniline substituted di-SNS derivative, producing a well-ordered cross-linked polymer matrix, which leads to an enhanced electron transfer rate during the doping/dedoping process.<sup>191</sup> Furthermore, a multi-electrochromic behavior, from purple to light blue, was observed as a function of the applied potential.

### Organic solar cells

Due to their outstanding optoelectronic properties, conducting polymers have become classic materials for the design of photovoltaic devices such as dye-sensitized solar cells (DSSCs), organic solar cells (OSCs), and perovskite solar cells (PSCs).

Electropolymerized  $\pi$ -conjugated polymers are commonly used in solar cells as anodic/cathodic interlayers<sup>192,193</sup> or hole-/electron-transporting layers.<sup>194,195</sup> In such applications, PEDOT doped with PSS is the most used conducting polymer due to its unique electric and optical properties in synergy with its aqueous solution-processability.<sup>196–201</sup> However, multiple efforts have been carried out to improve the performance of such devices. For example, it has been demonstrated that electrochemical polymerization allows fine-tuning of the thickness and morphology of the film, which impacts the performance of photovoltaic devices.<sup>202,203</sup> Alternatively, a synergistic effect between the alkoxy thiophene's chemical structure and these systems' performance has been extensively studied.<sup>204–207</sup> For example, poly-spirobipropylene-dioxythiophene (poly-spiroBiProDOT) has been used as a counter electrode as an alternative of electrocatalytic platinum in solar cells.<sup>208</sup> Due to its ordered thiophenic structure, poly-spiroBiProDOT exhibits better charge transfer than PEDOT, which increases the photocurrent density and as a consequence, the cell efficiency. Reynolds *et al.* studied the impact of the placement, design and branching point of side chains present in dialkoxy-functionalized thiophenes on the photostability of conducting polymers.<sup>209</sup> An enhanced photostability was obtained for non-branched dialkoxy-thiophenes in comparison with branched and cross-linked alkyl substituents.

Electropolymerized PEDOT functionalized with  $\text{C}_{60}$  fullerene has been used as a selective contact and transparent electron-conducting layer in perovskite solar cells. The fullerene moiety acts as a strong electron acceptor, translating into a four-fold improved energy conversion efficiency compared to the device with pristine PEDOT.<sup>210</sup> Kuway *et al.* used a core of alkoxy-substituted thiophene derivatives, connected to fluorinated 1,1-dicyanomethylene-3-indanone (DFIC) terminals for the design of organic solar cells based on near-infrared (NIR) (Fig. 5a).<sup>211</sup> In particular, the presence of a non-cyclic alkoxy thiophene core led to a blue-shifted absorption and an elevated LUMO level; this resulted in a good conversion efficiency



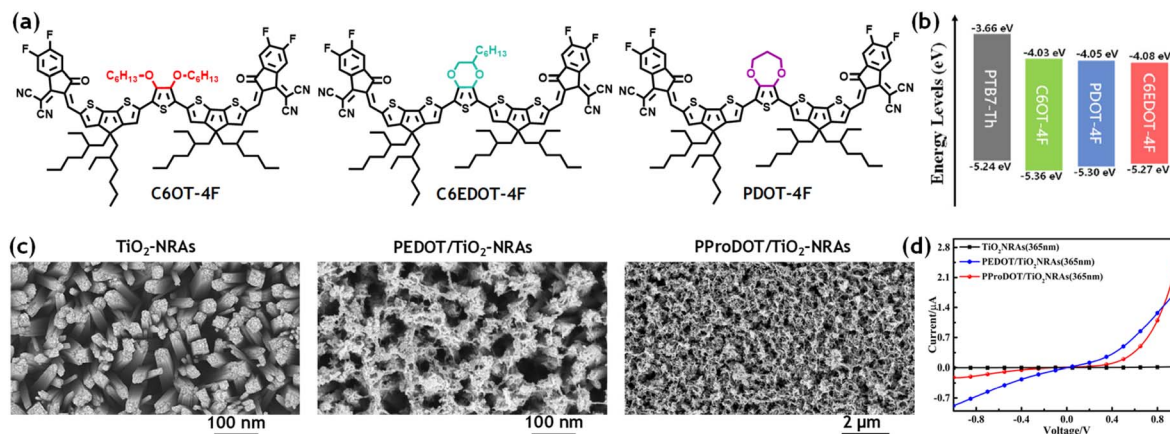


Fig. 5 (a) Chemical structures of alkoxy substituted thiophene derivatives connected to fluorinated 1,1-dicyanomethylene-3-indanone groups: C6OT-4F, C6EDOT-4F, and PDOT-4F. (b) Energy level diagram of PTB7-Th and its comparison with the corresponding electron ring acceptors. Adapted from ref. 211 with permission from Elsevier, copyright 2022. (c) SEM images of the top view of  $TiO_2$  NRAs (left) PEDOT/TiO<sub>2</sub>-NRAs (center) and PProDOT/TiO<sub>2</sub>-NRAs (right). (d)  $I-V$  curves of  $TiO_2$ -NRAs, PEDOT/TiO<sub>2</sub>-NRAs and PProDOT/TiO<sub>2</sub>-NRAs illuminated by 365 nm UV light. Adapted from ref. 223 with permission from Elsevier, copyright 2021.

(9.83%), with a low energy loss of 0.47 eV, which is relatively low in comparison with that of alternative NIR based organic solar cells (Fig. 5b). In addition to this approach, the study of the nanostructure of the electrode surface impacting the performance of photovoltaic devices has been conducted. For example, organic photovoltaic devices based on PEDOT:PPS deposited on copper nanowires exhibit an outstanding power conversion efficiency of 17.6%.<sup>212</sup> With a similar philosophy,  $TiO_2$  nanorod arrays (NRAs), modified electrochemically with PEDOT or PProDOT, present an efficient photocurrent performance (Fig. 5c and d).<sup>213</sup> The three-dimensional porous network structure of the  $TiO_2$  nanorod arrays increases the contact surface during electropolymerization, which leads to a larger p-n heterojunction. Moreover, by fine-tuning the polymeric nanofibril geometry it is possible to enhance the efficiency of organic solar cells.<sup>214,215</sup> The incorporation of 3,4-alkoxythiophene with different alkyl side chain lengths on the polymeric donor layer regulates the lamellar stacking, producing fibril structures with different diameters (from 12 nm to 28 nm). The formation of such structures promotes fibrillary charge transport which is reflected in enhanced power conversion efficiencies (above 18%).

## Electroanalytical applications

In the field of electroanalysis, electrogenerated CPs are interesting materials due to their large intrinsic contact area, intrinsic porosity, efficient conductivity, and wide electroactive window.<sup>94</sup> Furthermore, by fine-tuning the chemical structure of the polymer, it is possible to produce an intrinsic surface enrichment caused by physicochemical interactions between the desired analyte and the heteroatoms within the monomeric structure. The synergy between these ingredients leads to a considerable increase in sensitivity and selectivity compared to classic electrodes. In this context, 3,4-alkoxy thiophenes have been widely used to analyze different organic and inorganic

probes efficiently. For example, PEDOT and substituted-PEDOT modified electrodes exhibit relatively good detection limits, in the range between ppb and ppm, for multiple metal ions, *e.g.*,  $Na^+$ ,  $Hg^{2+}$ ,  $Zn^{2+}$ ,  $Pb^{2+}$ ,  $As^{3+}$ ,  $Cu^{2+}$ ,  $Cd^{2+}$ ,  $Ag^+$  and  $Ca^{2+}$ .<sup>216–220</sup> More recently, highly ordered macroporous electrodes made of

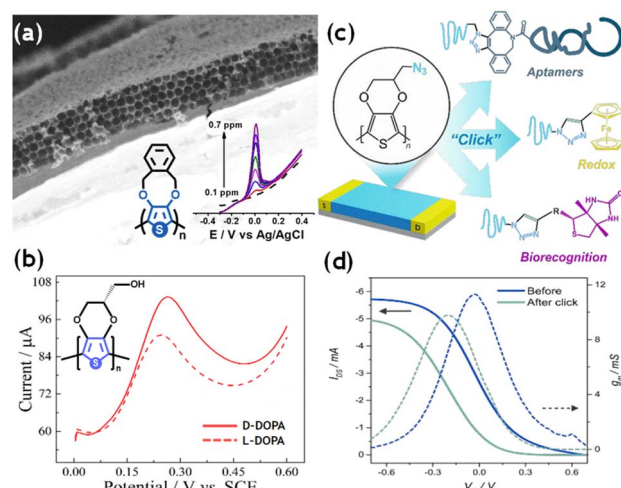


Fig. 6 (a) SEM image of the cross-section of a highly ordered macroporous PXDOT electrode. Insets show a square wave anodic stripping voltammetry obtained during the successive addition of  $Cu^{2+}$  in a 10% diluted mezcal solution. Adapted from ref. 221 with permission from the American Chemical Society, copyright 2018. (b) Differential pulse voltammograms of (S)-PEDOT modified electrodes in a solution containing D- or L-DOPA. Adapted from ref. 223 with permission from The American Chemical Society, copyright 2017. (c) Chemical structure of the poly-azidomethyl-EDOT (PEDOT-N<sub>3</sub>) deposited between the drain and source electrodes to generate OECTs, and the schematic representation of the possible click functionalization with redox probes and biorecognition elements. (d) Threshold voltage and maximum transconductance for a PEDOT-N<sub>3</sub> OECT before and after the click reaction with ethynyl-ferrocene. Adapted from ref. 239 with permission from The American Chemical Society, copyright 2022.

PXDOT were designed. With their unique design, these electrodes could efficiently quantify  $\text{Cu}^{2+}$  in commercial alcoholic spirituous beverages (Fig. 6a).<sup>221</sup> The formation of porous structures within CPs improves the ion transport inside the polymer matrix. It increases the contact surface, causing an enhancement of the sensitivity and the response time of the electrodes. In the past decade, the use of 3,4-alkoxythiophenes has also been extended to chiral electroanalysis. Enantioselective polymers were designed by introducing chiral moieties such as hyaluronic acid and anionic collagen as counter ions during electropolymerization or by carrying out the electrochemical deposition in a chiral solid phase, such as hydroxypropyl cellulose (HPC). These materials have been used for the enantioselective discrimination of (R)-(−)- and (S)-(+) -mandelic acid in aqueous solution.<sup>222</sup> With a similar philosophy, Dong *et al.* designed enantioselective electrochemical sensors through two different EDOT derivatives: (2R)-(2,3-dihydrothieno[3,4-*b*][1,4]dioxin-2-yl)methanol ((R)-EDTM) and (2S)-(2,3-dihydrothieno[3,4-*b*][1,4]dioxin-2-yl)methanol ((S)-EDTM) for the efficient recognition of *D*- and *L*-3,4-dihydroxyphenylalanine (DOPA) (Fig. 6b).<sup>223</sup>

The various efforts to develop novel and straightforward electroanalytical applications based on poly (3,4-alkoxythiophene) systems have also led to their use in organic electrochemical transistors (OECTs).<sup>224–226</sup> These devices consist of an organic channel, a gate, and reference electrodes. Applying a voltage between the gate and channel electrodes (gate voltage,  $V_G$ ) induces a current flow across the organic transistor (drain current,  $I_D$ ) limited by the exchange of ions between the electrolyte and the channel. Thus, in theory, the OECTs transform relatively small  $V_G$  changes into large  $I_D$  variations through the  $\pi$ -conjugated polymer located in the channel. The reader is invited to consult other publications for a more detailed description of this technique.<sup>227,228</sup> In particular, the organic conductor must present easy ionic exchange, fast and reversible charge/discharge transitions, and efficient charge storage operation (high volumetric capacitance). Among all the different types of conducting polymers, poly (3,4-alkoxythiophenes), particularly PEDOT, fulfills these requirements. Since the efficiency of the OECT is intimately related to the mixed conductivity of the polymer, it is possible to improve the performance of the device by fine-tuning either the structure of the doping counter ion<sup>229,230</sup> or the  $\pi$ -conjugated polymer.<sup>231–233</sup> For example, it has been demonstrated that by functionalizing EDOT and ProDOT with polar side chains, it is possible to enhance the ion and electron mobility within the polymeric matrix.<sup>234,235</sup> OECTs designed with these modified alkoxothiophenes exhibit efficient hole mobility and volumetric capacitance with high stability (up to 500 cycles). With the same philosophy, one can selectively target chemical analytes of interest. Cloutet *et al.* designed a cation-selective polyelectrolyte, poly-4-styrene sulfonyl (phenyl-18-crown-6)imide.<sup>236</sup> The crown ether moiety is a cation scavenger targeting  $\text{K}^+$  ions, conferring the PEDOT: P(STFSIco-S(18-crown-6)) films with cation selectivity. With a similar approach, copolymers of EDOT and crown ether-modified thiophenes allow the design of ion-selective OECTs, where the electric readout signal is

a function of the type of cation (*i.e.*,  $\text{Na}^+$  and  $\text{K}^+$ ) and its concentration.<sup>237</sup> Recently, an EDOT-based trimer, modified with a dipicolylamine (DPA) group, was electropolymerized and used to build OECTs for the selective detection and quantification of  $\text{Zn}^{2+}$  cations.<sup>238</sup> Finally, Knoll *et al.* proposed a “clickable” OECT, based on azidomethyl-EDOT (Fig. 6c) or ethynyl-EDOT.<sup>239,240</sup> The obtained transistors present lower threshold voltages than alternative PEDOT-based devices, with maximum transconductance voltage values close to 0 V (Fig. 6d). More importantly, the azide and ethynyl moieties enable the functionalization of the obtained transistor with alkyne-bearing molecules, such as redox probes, biorecognition elements, and gelatin macrostructures, thereby expanding the capabilities of the OECT to alternative transistor-based biosensors and enhancing biocompatibility for cell interfacing.

### Unconventional approaches

Finally, in recent years, attempts have been made to couple the outstanding properties of 3,4-alkoxythiophenes with bipolar electrochemistry (BE). Briefly, BE is an interesting alternative to induce wireless asymmetric polarization along a conducting object, or a bipolar electrode (BPE), present in an electrolyte, but without physical connection to an electrode.<sup>241–243</sup> This can be achieved by applying a high enough electric field ( $\epsilon$ ), which produces a polarization potential difference ( $\Delta V$ ) between the

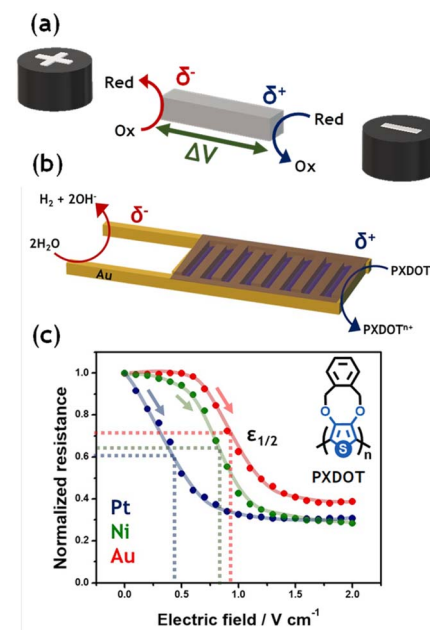


Fig. 7 (a) Schematic illustration of the fundamental concept of bipolar electrochemistry (BE) with a representation of the induction of redox reactions at both extremities of the bipolar electrode (BPE). (b) Schematic illustration of the modified IDME BPE, indicating the associated chemical reactions. The yellow and purple parts represent the interdigitated structure and PXDOT, respectively. (c) Normalized resistance plot as a function of the applied electric field for evaluating HER activity of Pt-, Au-, and Ni/Au-PXDOT IDME BPEs (blue, red, and green dots, respectively). Adapted from ref. 261 with permission from Elsevier, copyright 2023.



extremities of the BPE (Fig. 7a). In the presence of electroactive species, it is possible to trigger redox reactions at each side of the BPE when the  $\Delta V$  overcomes the reactions' thermodynamic threshold potential ( $\Delta V_{\min}$ ). This approach has gained considerable attention in applications ranging from electroanalysis to electrosynthesis.<sup>244–249</sup> For a more detailed description of this rather unconventional electrochemical concept, it is suggested that the reader consult specialized reviews.<sup>241–247</sup>

Bipolar electrochemistry has been used as a powerful tool to modify conducting substrates with poly-3,4-alkoxythiophenes asymmetrically. Inagi's group has extensively studied the wireless electropolymerization of PEDOT employing this method. In brief, by applying an appropriate electric field, the oxidation of EDOT and the reduction of a sacrificial compound, *i.e.* quinone, occur at the anodic and cathodic extremities of the BPE, respectively. Furthermore, fine-tuning of the experimental setup enables the possible electrosynthesis of well-defined macroscopic polymers. For example, PEDOT microfiber networks have been obtained through alternating current bipolar electropolymerization, which involves controlling the frequency, type of solvent, and electrolyte.<sup>250,251</sup> Similarly, Pt-PEDOT Janus wires, in-plane PEDOT films, and fibers were obtained.<sup>252–254</sup> PEDOT's template-free perpendicular growth was obtained using a bipolar electrochemical setup. In this case, the spatial distribution of the feeder electrodes, coupled with alternating current polymerization, enables the formation of polymeric fiber arrays.<sup>255</sup> This approach enables the generation of polymeric films with anisotropic electrical behaviour due to the formation of conductivity and composition gradients along the films.<sup>254,256</sup> Förster *et al.* demonstrated the possible region-selective deposition of PEDOT by taking advantage of an array of multiple feeder electrodes with different spatial distributions.<sup>257,258</sup> This approach enables the efficient mapping of the electric field distribution across the BPE by altering the coloration or thickness of the deposited conducting polymer.<sup>259</sup>

Besides, the potential of BE for the asymmetric functionalization of conductive objects has been recently explored. For example, free-standing PEDOT wires have been used as a BPE to design light-emitting self-propelled devices.<sup>260</sup> In this approach, the electrogenerated chemiluminescence of luminol occurs at the anodic side of the CP wire, whereas at the cathodic side, hydrogen peroxide reduction occurs. The generation of oxygen triggers the self-propulsion of such objects due to the intrinsic breaking of symmetry. Finally, the synergy between the conducting/insulating transition of 3,4-alkoxythiophenes and BE was used to design a wireless method to evaluate the electrocatalytic activity of metallic surfaces towards hydrogen and oxygen evolution reactions.<sup>261</sup> In this work, a PXDOT-modified interdigitated microelectrode (IDME) was used as a bipolar electrode, where the insulating/conducting transition of the polymer acts as a variable-resistance switch. In contrast, water splitting takes place on the opposite side of the BPE (Fig. 7b). The electrocatalytic activity of Pt, Au, and Ni was expressed in terms of the half-wave electric field, showing good agreement with the characteristic trend of these metals toward water-splitting reactions obtained using more traditional electrochemical tools, such as cyclic voltammetry (Fig. 7c).

## Conclusions

The remarkable properties of poly-(3,4-alkoxythiophenes) compared to other families of conducting polymers have triggered intense research over the last few decades and can be considered a first-choice material for developing new applications. They offer a balance between electrical conductivity, stability, mechanical properties, and tunable chemical properties. The synthesis of the corresponding monomers produces custom-made materials with specific physical and chemical properties. This task can be achieved through diverse synthetic pathways, which are part of molecular and polymer engineering, generating significant molecular diversity to explore the most suitable material for a specific application. Such fine-tuning of these physicochemical features enabled an understanding of the relationship between the structure and response properties, a knowledge development highly appreciated by the materials chemistry community. This control is achieved by selecting adequate polymer properties that are reflected in the macroscopic behavior, such as inter- and intra-chain interactions, band gap, and doping level. Among the emerging and recent technologies, organic batteries and capacitors benefit from their reversible redox capacity, which requires fast kinetics for charge and discharge, as well as electrochemical and chemical stability, to continue progress in this field. Applications in organic electronics primarily benefit from the conductive properties of these materials, which are controlled by the doping level and band gap. As an example of future directions, post-processing the lateral chain to expose hydroxyl groups resulted in an increase in the conductivity of the PEDOT derivative to values close to  $700 \text{ S cm}^{-1}$  through a simple chemical process; with an additional thermal step, the conductivity reaches values averaging  $1100 \text{ S cm}^{-1}$ .<sup>145</sup> A key consideration is the potential recyclability-degradability of these materials,<sup>262,263</sup> which would facilitate the use of sustainable materials in applications. This review demonstrates that imagination is the only limit in the field of conducting polymers, and many interesting and novel materials based on 3,4-alkoxythiophenes will undoubtedly continue to be developed in the future. Emerging applications such as biochemical sensing,<sup>264,265</sup> imaging,<sup>266,267</sup> wearable devices<sup>268,269</sup> or electrocatalysis,<sup>270–272</sup> nowadays use this polymer family. Moreover, the synergistic effect between wireless electrochemistry and the properties of poly-3,4-alkoxythiophenes has paved the way for novel applications in cell stimulation<sup>273</sup> and drug delivery.<sup>274</sup> Strategies to increase the amount of charge carriers, without suffering from chemical or electrochemical degradation, or an increase in processability, require the exploration of new substituents and strategies to achieve a long-range order of chains, which is forecast to be very promising for future members of the poly-(3,4-alkoxythiophenes).

## Data availability

No new data were obtained and the contained information comes from available bibliographical references.



## Author contributions

F. A. B.-P.: investigation, data curation & writing – original draft; M. P. F.-M.: investigation, data curation & writing – original draft; A. K.: review & editing; G. S.: conceptualization, methodology, supervision, validation, writing – reviewing & editing and B. A. F.-U.: conceptualization, funding acquisition, supervision, validation, writing – reviewing & editing.

## Conflicts of interest

There are no conflicts to declare.

## Acknowledgements

The authors thank M. E. Citlalit Martínez-Soto for the technical support. This research was conducted with the support of the CONAHCYT project A1-S-18230 and the project PAPIIT-DGAPA UNAM IV20222. Support by the ANR project CHIRASENSEO (ANR-23-CE42-0004-01) is also acknowledged.

## References

- 1 H. Shirakawa, A. McDiarmid and A. Heeger, *Chem. Commun.*, 2003, **4**, 1–4.
- 2 X. Guo and A. Facchetti, *Nat. Mater.*, 2020, **19**, 922–928.
- 3 T. M. Swager, *Macromolecules*, 2017, **50**, 4867–4886.
- 4 J. Heinze, B. A. Frontana-Uribe and S. Ludwigs, *Chem. Rev.*, 2010, **110**, 4724–4771.
- 5 R. Shomura, K. Sugiyasu, T. Yasuda, A. Sato and M. Takeuchi, *Macromolecules*, 2012, **45**, 3759–3771.
- 6 G. Pace, I. Bargigia, Y. Y. Noh, C. Silva and M. Caironi, *Nat. Commun.*, 2019, **10**, 5226.
- 7 G. Salinas and B. A. Frontana-Uribe, *Chemelectrochem*, 2019, **6**, 4105–4117.
- 8 J. G. Ibanez, M. E. Rincon, S. Gutierrez-Granados, M. Chahma, O. A. Jaramillo-Quintero and B. A. Frontana-Uribe, *Chem. Rev.*, 2018, **118**, 4731–4816.
- 9 G. Barbarella, M. Melucci and G. Sotgiu, *Adv. Mater.*, 2005, **17**, 1581–1593.
- 10 L. Groenendaal, F. Jonas, D. Freitag, H. Pielartzik and J. R. Reynolds, *Adv. Mater.*, 2000, **12**, 481–494.
- 11 L. Groenendaal, G. Zotti, P. H. Aubert, S. M. Waybright and J. R. Reynolds, *Adv. Mater.*, 2003, **15**, 855–879.
- 12 Y. Wang, *J. Phys.:Conf. Ser.*, 2009, **152**, 012023.
- 13 O. Hinsberg, *Ber. Dtsch. Chem. Ges.*, 1910, **43**, 901–906.
- 14 E. W. Fager, *J. Am. Chem. Soc.*, 1945, **67**, 2217–2218.
- 15 D. J. Chadwick, J. Chambers, G. D. Meakins and R. L. Snowden, *J. Chem. Soc., Perkin Trans.*, 1972, **1**, 2079–2081.
- 16 V. N. Gogte, L. G. Shah, B. D. Tilak, K. N. Gadekar and M. B. Sahasrabudhe, *Tetrahedron*, 1967, **23**, 2437–2441.
- 17 M. Coffey, B. R. McKellar, B. A. Reinhardt, T. Nijakowski and W. A. Feld, *Synth. Commun.*, 1996, **26**, 2205–2212.
- 18 F. Dallacker and V. Mues, *Chem. Ber.*, 1975, **108**, 569–575.
- 19 F. Dallacker and V. Mues, *Chem. Ber.*, 1975, **108**, 576–581.
- 20 A. Merz, C. Rehm and J. fur Prakt, *J. Praktische Chem., Chemiker-Zeitung*, 1996, **338**, 672–674.
- 21 M. A. Al-jumaili and S. Woodward, *Tetrahedron*, 2017, **73**, 5847–5852.
- 22 F. Von Kieseritzky, F. Allared, E. Dahlstedt and J. Hellberg, *Tetrahedron Lett.*, 2004, **45**, 6049–6050.
- 23 S. Das, P. K. Dutta, S. Panda and S. S. Zade, *J. Org. Chem.*, 2010, **75**, 4868–4871.
- 24 A. R. Agrawal, N. R. Kumar, S. Debnath, S. Das, C. Kumar and S. S. Zade, *Org. Lett.*, 2018, **20**, 4728–4731.
- 25 K. Zong, L. Madrigal and J. R. Reynolds, *Chem. Commun.*, 2002, 2498–2499.
- 26 D. Caras-Quintero and P. Bauerle, *Chem. Commun.*, 2002, 2690–2691.
- 27 L. Zuo, F. L. Qing, W. D. Meng, X. Huang, S. Zhang, Q. Wu and J. Fluor, *Chem.*, 2004, **125**, 1441–1446.
- 28 T. Tsunoda, Y. Yamamiya, Y. Kawamura and S. Itô, *Tetrahedron Lett.*, 1995, **36**, 2529–2530.
- 29 Z. Xu, J. H. Kang, F. Wang, S. M. Paek, S. J. Hwang, Y. Kim, S. J. Kim, J. H. Choy and J. Yoon, *Tetrahedron Lett.*, 2011, **52**, 2823–2825.
- 30 D. Caras-Quintero and P. Bäuerle, *Chem. Commun.*, 2004, **4**, 926–927.
- 31 K. Krishnamoorthy, A. V. Ambade, M. Kanungo, A. Q. Contractor and A. Kumar, *J. Mater. Chem.*, 2001, **11**, 2909–2911.
- 32 T. Darmanin, E. L. Klimareva, I. Schewtschenko, F. Guittard and I. F. Perepichka, *Macromolecules*, 2019, **52**, 8088–8102.
- 33 A. Martinelli, A. Nitti, R. Po and D. Pasini, *J. Org. Chem.*, 2024, **89**, 4237–4243.
- 34 B. D. Reeves, B. C. Thompson, K. A. Abboud, B. E. Smart and J. R. Reynolds, *Adv. Mater.*, 2002, **14**, 717–719.
- 35 J. Arias-Pardilla, P. A. Giménez-Gómez, A. De La Peña, J. L. Segura and T. F. Otero, *J. Mater. Chem.*, 2012, **22**, 4944–4952.
- 36 P. Leriche, P. Blanchard, P. Frère, E. Levillain, G. Mabon and J. Roncali, *Chem. Commun.*, 2006, 275–277.
- 37 D. L. Tarange, N. Nayak and A. Kumar, *Org. Process Res. Dev.*, 2023, **27**, 358–366.
- 38 B. A. Frontana-Uribe and J. Heinze, *Tetrahedron Lett.*, 2006, **47**, 4635–4640.
- 39 E. V. Ganin, S. S. Basok, A. A. Yavolovskii, M. M. Botoshansky and M. S. Fonari, *CrystEngComm*, 2011, **13**, 674–683.
- 40 P. A. Cisneros-Pérez, B. A. Frontana-Uribe, D. Martínez-Otero and E. Cuevas-Yáñez, *Tetrahedron Lett.*, 2016, **57**, 5089–5093.
- 41 M. P. Krompiec, S. N. Baxter, E. L. Klimareva, D. S. Yufit, D. G. Congrave, T. K. Britten and I. F. Perepichka, *J. Mater. Chem. C*, 2018, **6**, 3743–3756.
- 42 A. Kumar, D. M. Walsh, M. C. Morvant, F. Piroux, K. A. Abboud and J. R. Reynolds, *Chem. Mater.*, 1998, **10**, 896–902.
- 43 J. Zhao, X. Gou, C. Hua and L. Wang, *Chin. J. Catal.*, 2012, **33**, 1262–1265.
- 44 P. A. Cisneros-Pérez, D. Martínez-Otero, E. Cuevas-Yáñez and B. A. Uribe-Frontana, *Synth. Commun.*, 2014, **44**, 222–230.



45 J. M. Barker, P. R. Huddleston and M. L. Wood, *Synth. Commun.*, 1975, **5**, 59–64.

46 S. Sreekumar, S. Xavier, A. Govindan, R. E. Thampikannu, K. Vellayan and B. González, *Res. Chem. Intermed.*, 2020, **46**, 4529–4542.

47 P. M. Dicarmine, T. B. Schon, T. M. McCormick, P. P. Klein and D. S. Seferos, *J. Phys. Chem. C*, 2014, **118**, 8295–8307.

48 F. D'Amico, C. Papucci, D. Franchi, G. Reginato, M. Calamante, L. Zani, A. Dessi and A. Mordini, *ACS Sustainable Chem. Eng.*, 2022, **10**, 3037–3047.

49 G. A. Sotzing, J. R. Reynolds and P. J. Steel, *Chem. Mater.*, 1996, **8**, 882–889.

50 A. Ulman and J. Manassen, *J. Chem. Soc. Perkin Trans.*, 1979, **1**, 1066–1069.

51 N. Agarwal, C. H. Hung and M. Ravikanth, *Tetrahedron*, 2004, **60**, 10671–10680.

52 A. K. Mohanakrishnan, A. Hucke, M. A. Lyon, M. V. LakshmiKantham and M. P. Cava, *Tetrahedron*, 1999, **55**, 11745–11754.

53 K. Wang, T. Zhang, Y. Hu, W. Yang and Y. Shi, *Electrochim. Acta*, 2014, **130**, 46–51.

54 I. Stolić, K. Miskovic, A. Magdaleno, A. M. Silber, I. Piantanida, M. Bajic and L. Glavas-Obravac, *Bioorg. Med. Chem.*, 2009, **17**, 2544–2554.

55 Y. Lu, Y. P. Wen, B. Y. Lu, X. M. Duan, J. K. Xu, L. Zhang and Y. Huang, *Chin. J. Polym. Sci.*, 2012, **30**, 824–836.

56 S. Akoudad and J. Roncali, *Electrochem. Commun.*, 2000, **2**, 72–76.

57 I. F. Perepichka, E. Levillain and J. Roncali, *J. Mater. Chem.*, 2004, **14**, 1679–1681.

58 K. Krishnamoorthy, M. Kanungo, A. Q. Contractor and A. Kumar, *Synth. Met.*, 2001, **124**, 471–475.

59 J. L. Segura, R. Gómez, E. Reinold and P. Bäuerle, *Org. Lett.*, 2005, **7**, 2345–2348.

60 L. Dong, B. Lu, X. Duan, J. Xu, D. Hu, K. Zhang, X. Zhu, H. Sun, S. Ming, Z. Wang and S. Zhen, *J. Polym. Sci. Part A Polym. Chem.*, 2015, **53**, 2238–2251.

61 C. J. Kousseff, F. E. Taifakou, W. G. Neal, M. Palma and C. B. Nielsen, *J. Polym. Sci.*, 2022, **60**, 504–516.

62 P. Sitarik, S. S. Nagane, S. Chhatre, Y. Wu, Q. Baugh and D. C. Martin, *Mater. Adv.*, 2022, **3**, 6037–6049.

63 M. Sassi, L. Mascheroni, R. Ruffo, M. M. Salamone, G. A. Pagani, C. M. Mari, G. D'Orazio, B. La Ferla and L. Beverina, *Org. Lett.*, 2013, **15**, 3502–3505.

64 D. Mantione, N. Casado, A. Sanchez-Sanchez, H. Sardon and D. Mecerreyes, *J. Polym. Sci. Part A Polym. Chem.*, 2017, **55**, 2721–2724.

65 J. Kang, K. Zong and Y. S. Lee, *React. Funct. Polym.*, 2024, **205**, 106063.

66 N. Nayak, K. Arora, S. Shirke, S. Shriwardhankar and A. Kumar, *Eur. Polym. J.*, 2022, **178**, 111436.

67 B. T. Ditullio, L. R. Savagian, O. Bardagot, M. De Keersmaecker, A. M. Österholm, N. Banerji and J. R. Reynolds, *J. Am. Chem. Soc.*, 2023, **145**, 122–134.

68 J. F. Ponder Jr, S. A. Gregory, A. Atassi, A. K. Menon, A. W. Lang, L. R. Savagian, J. R. Reynolds and S. K. Yee, *J. Am. Chem. Soc.*, 2022, **144**, 1351–1360.

69 M. M. Durbin, A. H. Balzer, J. R. Reynolds, E. L. Ratcliff, N. Stingelin and A. M. Österholm, *Chem. Mater.*, 2024, **36**, 2634–2641.

70 W. Wu, S. Yu, D. S. Forbes, H. Jiang, M. Ahmed and J. Mei, *J. Am. Chem. Soc.*, 2024, **146**, 578–585.

71 S. Cosnier and A. Karyakin, *Electropolymerization: Concepts, Materials and Applications*, Wiley-VCH, Weinheim, Germany, 2010.

72 K. A. Kurdi, S. A. Gregory, M. P. Gordon, J. F. Ponder Jr, A. Atassi, J. M. Rinehart, A. L. Jones, J. J. Urban, J. R. Reynolds, S. Barlow, S. R. Marder and S. K. Yee, *ACS Appl. Mater. Interfaces*, 2022, **14**, 29039–29051.

73 P. Sakunpongpitiporn, K. Phasuksom, N. Paradee and A. Sirivat, *RSC Adv.*, 2019, **9**, 6363–6378.

74 W. Lövenich, *Polym. Sci., Ser. C*, 2014, **56**, 135–143.

75 B. Winther-Jensen and K. West, *Macromolecules*, 2004, **37**, 4538–4543.

76 C. Jiang, G. Chen and X. Wang, *Synth. Met.*, 2012, **162**, 21–22.

77 Y. Zhang and K. S. Suslick, *Chem. Mater.*, 2015, **27**, 7559–7563.

78 S. Zhang, W. Zhang, G. Zhang, Y. Bai, S. Chen, J. Xu, Z. Yu and K. Sun, *Mater. Lett.*, 2018, **222**, 105–108.

79 T. Zubair, R. S. Ramos, A. Morales and R. M. Pankow, *Polym. Chem.*, 2025, **16**, 1188–1196.

80 A. Kumar, R. Singh, S. P. Gopinathan and A. Kumar, *Chem. Commun.*, 2012, **48**, 4905–4907.

81 B. C. Thompson, Y. G. Kim, T. D. McCarley and J. R. Reynolds, *J. Am. Chem. Soc.*, 2006, **128**, 12714–12725.

82 N. Gulprasertat, J. Chapromma, T. Aree and Y. Sritana-Anant, *J. Appl. Polym. Sci.*, 2015, **132**, 42233.

83 D. Bhardwaj, S. Gupta, A. Mishra, S. Singhal, Shahjad, M. Balkhandia, R. Sharma and A. Patra, *J. Polym. Res.*, 2023, **30**, 53.

84 W. Lu, J. Kuwabara, M. Kuramochi and T. Kanbara, *J. Polym. Sci. Part A Polym. Chem.*, 2015, **53**, 1396–1402.

85 J. F. Ponder, B. Schmatz, J. L. Hernandez and J. R. Reynolds, *J. Mater. Chem. C*, 2018, **6**, 1064–1070.

86 C. Beaumont, T. Lemieux, S. Aivali, M. H. Sangachin, A. Gasonoo, T. M. St-Pierre, M. Belanger, S. Beaupre, G. C. Welch and M. Leclerc, *ACS Macro Lett.*, 2024, **13**, 1133–1138.

87 J. F. Berbigier, R. M. D'Souza, R. N. Bennett and T. L. Kelly, *ACS Appl. Polym. Mater.*, 2023, **5**, 5687–5695.

88 J. F. Berbigier and T. L. Kelly, *ACS Appl. Polym. Mater.*, 2024, **6**, 8318–8325.

89 Y. Choi, Y. Kim, Y. Moon, K. Hwang, J. Hong, Y. Kim and D. Y. Kim, *Macromolecules*, 2023, **56**, 3324–3333.

90 X. Zhang, A. G. MacDiarmid and S. K. Manohar, *Chem. Commun.*, 2005, 5328–5330.

91 M. G. Han and S. H. Foulger, *Chem. Commun.*, 2005, **1**, 3092–3094.

92 A. G. Sadekar, D. Mohite, S. Mulik, N. Chandrasekaran, C. Sotiriou-Leventis and N. Leventis, *J. Mater. Chem.*, 2012, **22**, 100–108.

93 I. Bargigia, L. R. Savagian, A. M. Österholm, J. R. Reynolds and C. Silva, *J. Am. Chem. Soc.*, 2021, **143**, 294–308.



94 G. Salinas and B. A. Frontana-Uribe, *Electrochem.*, 2022, **3**, 492–506.

95 R. Xiao, S. I. Cho, R. Liu and S. B. Lee, *J. Am. Chem. Soc.*, 2007, **129**, 4438–4489.

96 C. B. Tran, T. F. Otero, J. Travas-Sejdic, Q. B. Le and R. Kiefer, *Synth. Met.*, 2023, **299**, 117466.

97 M. Dietrich, J. Heinze, G. Heywang and F. Jonas, *J. Electroanal. Chem.*, 1994, **369**, 87–92.

98 H. Yamato, K. I. Kai, M. Ohwa, T. Asakura, T. Koshiba and W. Wernet, *Synth. Met.*, 1996, **83**, 125–130.

99 K. Krishnamoorthy, M. Kanungo, A. Q. Contractor and A. Kumar, *Synth. Met.*, 2001, **124**, 471–475.

100 K. Krishnamoorthy, M. Kanungo, A. V. Ambade, A. Q. Contractor and A. Kumar, *Synth. Met.*, 2001, **125**, 441–444.

101 J. L. Segura, R. Gómez, R. Blanco, E. Reinold and P. Bäuerle, *Chem. Mater.*, 2006, **18**, 2834–2847.

102 F. Mouffouk and S. J. Higgins, *Electrochem. Commun.*, 2006, **8**, 15–20.

103 L. Vallan, E. Istif, I. J. Gomez, N. Alegret and D. Mantione, *Polymers*, 2021, **13**, 1977.

104 I. F. Perepichka, M. Besbes, E. Levillain, M. Salle and J. Roncali, *Chem. Mater.*, 2002, **14**, 449–457.

105 D. Mantione, E. Istif, G. Dufil, L. Vallan, D. Parker, C. Brochon, E. Cloutet, G. Hazioannou, M. Berggren, E. Stavrinidou and E. Pavlopoulou, *ACS Appl. Electron. Mater.*, 2020, **2**, 4065–4071.

106 V. Agrawal, D. Shahjad, D. Bhardwaj, R. Bhargav, G. D. Sharma, R. K. Bhardwaj, A. Patra and S. Chand, *Electrochim. Acta*, 2016, **192**, 52–60.

107 I. F. Perepichka, S. Roquet, P. Leriche, J. M. Raimondo, P. Frère and J. Roncali, *Chem. –Eur. J.*, 2006, **12**, 2960–2966.

108 E. Istif, D. Mantione, L. Vallan, G. Hazioannou, C. Brochon, E. Cloutet and E. Pavlopoulou, *ACS Appl. Mater. Interfaces*, 2020, **12**, 8695–8703.

109 F. Piron, P. Leriche, G. Mabon, I. Grosu and J. Roncali, *Electrochem. Commun.*, 2008, **10**, 1427–1430.

110 N. Hergué and P. Frère, *Org. Biomol. Chem.*, 2007, **5**, 3442–3449.

111 A. Berlin, G. Zotti, S. Zecchin, G. Schiavon, M. Cocchi, D. Virgili and C. Sabatini, *J. Mater. Chem.*, 2003, **13**, 27–33.

112 A. Berlin, G. Zotti, S. Zecchin, G. Schiavon, B. Vercelli and A. Zanelli, *Chem. Mater.*, 2004, **16**, 3667–3676.

113 H. Brisset, A. E. Navarro, C. Moustrou, I. F. Perepichka and J. Roncali, *Electrochem. Commun.*, 2004, **6**, 249–253.

114 N. Hergué, P. Leriche, P. Blanchard, M. Allain, N. Gallego-Planas, P. Frère and J. Roncali, *New J. Chem.*, 2008, **32**, 932–936.

115 G. Salinas, J. G. Ibanez, R. Vasquez-Medrano and B. A. Frontana-Uribe, *Synth. Met.*, 2018, **237**, 65–72.

116 G. Salinas, J. A. Del-Oso, P. J. Espinoza-Montero, J. Heinze and B. A. Frontana-Uribe, *Synth. Met.*, 2018, **245**, 135–143.

117 T. Nicolini, A. Villarroel Marquez, B. Goudeau, A. Kuhn and G. Salinas, *J. Phys. Chem. Lett.*, 2021, **21**, 10422–10428.

118 F. A. Bravo-Plascencia, M. P. Flores-Morales, G. Salinas and B. A. Frontana-Uribe, *Electrochim. Acta*, 2025, **511**, 145375.

119 T. Karazehir, B. Sarac, H. D. Gilsing, S. Gumrukcu, J. Eckert and A. S. Sarac, *Mol. Syst. Des. Eng.*, 2021, **6**, 214.

120 R. Schweiss, J. F. Lübben, D. Johannsmann and W. Knoll, *Electrochim. Acta*, 2005, **50**, 2849–2856.

121 X. Du and Z. Wang, *Electrochim. Acta*, 2003, **48**, 1713–1717.

122 M. Fall, L. Assogba, J. J. Aaron and M. M. Dieng, *Synth. Met.*, 2001, **123**, 365–372.

123 S. Akoudad and J. Roncali, *Electrochim. Commun.*, 2000, **2**, 72–76.

124 H. Sun, L. Zhang, L. Dong, X. Zhu, S. Ming, Y. Zhang, H. Xing, X. Duan and J. Xu, *Synth. Met.*, 2016, **211**, 147–154.

125 H. Goto and K. Akagi, *Chem. Mater.*, 2006, **18**, 255–262.

126 S. Matsushita, B. Yan, S. Yamamoto, Y. S. Jeong and K. Akagi, *Angew. Chem., Int. Ed.*, 2014, **53**, 1659–1663.

127 K. P. Prathish, R. C. Carvalho and C. M. A. Brett, *Electrochim. Commun.*, 2014, **44**, 8–11.

128 K. P. Prathish, R. C. Carvalho and C. M. A. Brett, *Electrochim. Acta*, 2016, **187**, 704–713.

129 M. Besbes, G. Trippe, E. Leviallain, M. Mazari, F. LeDerf, I. F. Perepichka, A. Derdour, A. Gorgues, M. Salle and J. Roncali, *Adv. Mater.*, 2001, **13**, 1249–1252.

130 B. Wei, L. Ouyang, J. Liu and D. C. Martin, *J. Mater. Chem. B*, 2015, **3**, 5028–5034.

131 A. E. Navarro, F. Fages, C. Moustrou, H. Brisset, N. Spinelli, C. Chaix and B. Mandrand, *Tetrahedron*, 2005, **61**, 3947–3952.

132 H. B. Bu, G. Gotz, E. Reinold, A. Vogt, R. Azumi, J. L. Segura and P. Bauerle, *Chem. Commun.*, 2012, **48**, 2677–2679.

133 J. Roncali, *Chem. Rev.*, 1997, **97**, 173–206.

134 J. Cameron, A. L. Kanibolotsky and P. J. Skabar, *Adv. Mater.*, 2024, **36**, 2302259.

135 H. Huang, L. Yang, A. Facchetti and T. J. Marks, *Chem. Rev.*, 2017, **117**, 10291–10318.

136 A. Giovannitti, D. T. Sbircea, S. Inal, C. B. Nilsen, E. Bandiello, D. A. Hanifi, M. Sessolo, G. M. Malliaras, I. McCulloch and J. Rivnay, *Proc. Natl. Acad. Sci. U. S. A.*, 2016, **113**, 12017–12022.

137 M. Casalegno, A. Famulari and S. V. Meille, *Macromolecules*, 2022, **55**, 2398–2412.

138 J. M. Rinehart, Z. Xu, Z. Wang, A. M. Österholm, L. Q. Flagg, L. J. Richter, C. R. Snyder, Y. Diao and J. R. Reynolds, *Chem. Mater.*, 2025, **37**(13), 4593–4606.

139 M. A. Ochieng, J. F. Ponder Jr and J. R. Reynolds, *Polym. Chem.*, 2020, **11**, 2173–2181.

140 K. Namsheer and C. S. Rout, *RSC Adv.*, 2021, **11**, 5659–5697.

141 I. E. Jacobs, Y. Lin, Y. Huang, X. Ren, D. Simatos, C. Chen, D. The, M. Statz, L. Lai, P. A. Finn, W. G. Neal, G. D'Avino, V. Lemaur, S. Fratini, D. Beljonne, J. Strzalka, C. B. Nielsen, S. Barlow, S. R. Marder, I. McCulloch and H. Sirringhaus, *Adv. Mater.*, 2022, **34**, 2102988.

142 *Semiconducting Polymers: Chemistry, Physics and Engineering*, ed. G. Hadzioannou and P. F. Van Hutten, Wiley-VCH Verlag GmbH, Weinheim, Germany, 1999.

143 R. K. Gupta. *Conducting Polymers*. Boca Raton (FL), CRC Press, 2022.

144 L. V. Kayser and D. J. Lipomi, *Adv. Mater.*, 2019, **31**, 1806133.



145 J. F. Ponder Jr, S. A. Gregory, A. Atassi, A. A. Advincula, J. M. Rinehart, G. Freychet, G. M. Su, S. K. Yee and J. R. Reynolds, *Angew. Chem., Int. Ed.*, 2023, **62**, e202211600.

146 A. M. Bryan, L. M. Santino, Y. Lu, S. Acharya and J. M. D'Arcy, *Chem. Mater.*, 2016, **28**, 5989–5998.

147 X. Wang, J. Zhou and W. Tang, *Mater. Horiz.*, 2021, **8**, 2373–2386.

148 D. Yuan, B. li, J. Cheng, Q. Guan, Z. Wang, W. Ni, C. Li, H. Liu and B. Wang, *J. Mater. Chem. A*, 2016, **4**, 11616–11624.

149 B. Li, J. Cheng, Z. Wang, Y. li, W. Ni and B. Wang, *J. Power Sources*, 2018, **376**, 117–124.

150 Y. Zhang, H. Zhang, S. Ming, P. Lin, R. Yu and T. Xu, *ACS Appl. Mater. Interfaces*, 2024, **16**, 22571–22579.

151 H. Wang, H. Yang, Y. Diao, Y. Lu, K. Chrulski and J. M. D'Arcy, *ACS Nano*, 2021, **15**, 7799–7810.

152 T. Karazehir, B. Sarac, H. D. Gilsing, J. Eckert and A. S. Sarac, *J. Electrochem. Soc.*, 2020, **167**, 070543.

153 Y. Liu, T. Abdiriyim, R. Jamal, X. Liu, N. Fan, M. Niyaz and Y. Zhang, *Appl. Surf. Sci.*, 2023, **608**, 154989.

154 I. Sahalianov, M. G. Say, O. S. Abdullaeva, F. Ahmed, E. Glowacki, I. Engquist, M. Berggren and I. Zozoulenko, *ACS Appl. Energy Mater.*, 2021, **4**, 8629–8640.

155 C. Strietzel, K. Oka, M. Strømme, R. Emanuelsson and M. Sjödin, *ACS Appl. Mater. Interfaces*, 2021, **13**, 5349–5356.

156 P. Das, B. Zayat, Q. Wei, C. Z. Salamat, I. B. Magdau, R. Elizalde-Segovia, D. Rawlings, D. Lee, G. Pace, A. Irshad, L. Ye, A. Schmitt, R. A. Segelman, T. F. Miller, S. H. Tolbert, B. S. Dunn, S. R. Narayan and B. C. Thompson, *Chem. Mater.*, 2020, **32**, 9176–9189.

157 P. Das, R. Elizalde-Segovia, B. Zayat, C. Z. Salamat, G. Pace, K. Zhai, R. C. Vincent, B. S. Dunn, R. A. Selgalman, S. H. Tolbert, S. R. Narayan and B. C. Thompson, *Chem. Mater.*, 2022, **34**, 2672–2686.

158 K. Oka, R. Löfgren, R. Emanuelsson, H. Nishide, K. Oyaizu, M. Strømme and M. Sjödin, *Chemelectrochem*, 2020, **7**, 3336–3340.

159 K. Oka, C. Strietzel, R. Emanuelsson, H. Nishide, K. Oyaizu, M. Strømme and M. Sjödin, *ChemSusChem*, 2020, **13**, 2280–2285.

160 N. Casado, G. Hernandez, A. Veloso, S. Devaraj, D. Mecerreyres and M. Armand, *ACS Macro Lett.*, 2016, **5**, 59–64.

161 P. O. Schwartz, M. Pejic, M. Wachtler and P. Bäuerle, *Synth. Met.*, 2018, **243**, 51–57.

162 H. Wang, R. Emanuelsson, H. Liu, F. Mamedov, M. Strømme and M. Sjödin, *Electrochim. Acta*, 2021, **391**, 138901.

163 K. Oka, C. Strietzel, R. Emanuelsson, H. Nishide, K. Oyaizu, M. Strømme and M. Sjödin, *Electrochem. Commun.*, 2019, **105**, 106489.

164 H. Wang, R. Emanuelsson, H. Liu, K. Edström, F. Mamedov, M. Strømme and M. Sjödin, *ACS Appl. Energy Mater.*, 2019, **2**, 7162–7170.

165 L. Åkerlund, R. Emanuelsson, G. Hernandez, M. Strømme and M. Sjödin, *J. Mater. Chem. A*, 2020, **8**, 12114–12123.

166 C. Strietzel, M. Sterby, H. Huang, M. Strømme, R. Emanuelsson and M. Sjödin, *Angew. Chem., Int. Ed.*, 2020, **59**, 9631–9638.

167 H. Huang, R. Emanuelsson, C. Karlsson, P. Jannasch, M. Strømme and M. Sjödin, *ACS Appl. Mater. Interfaces*, 2021, **13**, 19099–19108.

168 W. Hou, D. Tang, B. han, Y. Chen, C. Wang, Y. Liu, W. Chi, J. Chen, Y. Zhu, M. Ouyang, J. Liu and C. Zhang, *Chem. Eng. J.*, 2024, **497**, 154901.

169 J. Liu, W. Hou, D. Tang, Y. Gao, S. Yao, L. Jiang, Z. Zhang, M. Ouyang and C. Zhang, *ACS Sustainable Chem. Eng.*, 2022, **10**, 15978–15986.

170 S. Sinha, R. Daniels, O. Yassin, M. Baczkowski, M. Tefferi, A. Deshmukh, Y. Cao and G. Sotzing, *Adv. Meter. Technol.*, 2022, **7**, 2100548.

171 X. Xie, J. Yu, Z. Li, Z. Wu and S. Chen, *New J. Chem.*, 2022, **46**, 21167.

172 A. A. Advincula, A. L. Jones, K. J. Thorley, A. M. Österholm, J. F. Ponder Jr and J. R. Reynolds, *Chem. Mater.*, 2022, **34**, 4633–4645.

173 K. Perera, Z. Yi, L. You, Z. Ke and J. Mei, *Polym. Chem.*, 2020, **11**, 508.

174 N. Guven, H. Sultanova, B. Ozer, B. Yucel and P. Camurlu, *Electrochim. Acta*, 2020, **329**, 135134.

175 N. Guven, B. Yucel, H. Sultanova and P. Camurlu, *Dyes Pigm.*, 2022, **205**, 110526.

176 S. Ming, S. Zhen, H. Zhang, X. Han, Y. Zhang, J. Xu and J. Zhao, *Eur. Polym. J.*, 2022, **163**, 110938.

177 H. Chen, W. Wang, J. Zhu, J. Han and J. Liu, *Polymer*, 2022, **240**, 124485.

178 H. Chen, K. Lin, H. Liang, J. Tan, D. Zhou, X. Zhang, F. Liu and Y. Wang, *Synth. Met.*, 2022, **291**, 117200.

179 S. Sanchita, P. Yadav, S. Naqvi, S. Gupta and A. Patra, *ACS Omega*, 2019, **4**, 3484–3492.

180 E. G. C. Ergun and B. B. Carbas, *Polymer*, 2022, **256**, 125250.

181 C. Ernest, S. Fagour, X. Sallenave, P. H. Aubert and F. Vidal, *Adv. Mater. Technol.*, 2024, **9**, 2301654.

182 R. R. Ferreira, D. Mosca, T. Moreira, V. C. Wakchaure, G. Romano, A. Stopin, C. Pinheiro, A. M. T. Luci, L. M. A. Perdigao, G. Constantini, H. Amenitsch, C. A. T. Laia, A. J. Parola, L. Maggini and D. Bonifazi, *ACS Appl. Eng. Mater.*, 2024, **2**, 2640–2650.

183 G. Salinas, A. A. Villegas-Barron, J. Tadeo-Leon and B. A. Frontana-Uribe, *Electrochim. Acta*, 2023, **439**, 141673.

184 B. B. Carbas and E. G. C. Ergun, *Eur. Polym. J.*, 2022, **175**, 111363.

185 P. Camurlu, C. Gürtekin and Z. Bicil, *Electrochim. Acta*, 2012, **61**, 50–56.

186 T. Soganci, H. C. Soyleyici and M. Ak, *Phys. Chem. Chem. Phys.*, 2016, **18**, 14401–14407.

187 T. Soganci, S. Soyleyici, H. C. Soyleyici and M. Ak, *J. Electrochem. Soc.*, 2017, **164**, H11–H20.

188 E. G. C. Ergun and B. B. Carbas, *Mater. Today Commun.*, 2022, **32**, 103888.

189 E. Tutuncu, M. I. Ozkut, B. Balci, H. Berk and A. Cihaner, *Eur. Polym. J.*, 2019, **110**, 233–239.



190 J. L. Neto, L. P. A. da Silva, J. B. da Silva, A. J. C. da Silva, D. J. P. Lima and A. S. Ribeiro, *Synth. Met.*, 2020, **269**, 116545.

191 T. Nicolini, B. A. Frontana-Uribe, A. Kuhn and G. Salinas, *Chemelectrochem*, 2023, **10**, e202300346.

192 D. M. Montoya, E. Perez-Gutierrez, O. Barbosa-Garcia, W. Bernal, J. L. Maldonado, M. J. Percino, M. A. Meneses and M. Ceron, *Sol. Energy*, 2020, **195**, 610–617.

193 E. Marchini, M. Orlandi, N. Bazzanella, R. Boaretto, V. Cristino, A. Miotello, S. Caramori and S. Carli, *ACS Omega*, 2022, **7**, 29181–29194.

194 C. Anrango-Camacho, K. Pavon-Ipiales, B. A. Frontana-Uribe and A. Palma-Cando, *Nanomaterials*, 2022, **12**, 443.

195 J. Y. Shao and Y. W. Zhong, *ACS Sustainable Chem. Eng.*, 2022, **10**, 13555–13567.

196 Y. Jiang, T. Liu and Y. Zhou, *Adv. Funct. Mater.*, 2020, **30**, 2006213.

197 M. Zhu, K. Meng, C. Xu, J. Zhang and G. Ni, *Org. Electron.*, 2020, **78**, 105585.

198 E. Marchini, S. Caramori, C. A. Bignozzi and S. Carli, *Appl. Sci.*, 2021, **11**, 3795.

199 R. Bhargav, D. Bhardwaj, Shahjad, A. Patra and S. Chand, *ChemistrySelect*, 2016, **1**, 1347–1352.

200 S. Sandrez, Z. Molenda, C. Guyot, O. Renault, J. P. Barnes, L. Hirsch, T. Maindron and G. Wantz, *Adv. Electron. Mater.*, 2021, **7**, 2100394.

201 A. Gasonoo, C. Beaumont, A. Hoff, C. Xu, P. Egberts, M. Pahlevani, M. Leclerc and G. C. Welch, *Chem. Mater.*, 2023, **35**, 9102–9110.

202 J. A. Del-Oso, B. A. Frontana-Uribe, J. L. Maldonado, M. Rivera, M. Tapia-Tapia and G. Roa-Morales, *J. Solid State Electrochem.*, 2018, **22**, 2025–2037.

203 E. Nasibulin, S. Wei, M. Cox, I. Kymmissis and K. Levon, *J. Phys. Chem. C*, 2011, **115**, 4307–4314.

204 S. Lacher, N. Obata, S. C. Luo, Y. Matsuo, B. Zhu, H. H. Yu and E. Nakamura, *ACS Appl. Mater. Interfaces*, 2012, **4**, 3396–3404.

205 J. Marques dos Santos, M. Neophytou, A. Wiles, C. T. Howells, R. S. Ashraf, I. McCulloch and G. Cooke, *Dyes Pigm.*, 2021, **188**, 109152.

206 A. Mishra, S. Gupta and A. Patra, *J. Polym. Sci.*, 2022, **60**, 975–984.

207 Q. Mu, L. Feng, Z. Li, K. Fan, Q. Li, Z. Wei, Y. Cheng and B. Xu, *Sol. RRL*, 2024, **8**, 2400486.

208 M. C. Sil, H. D. Chang, J. J. Jhan and C. M. Chen, *J. Mater. Chem. C*, 2021, **9**, 12094.

209 D. E. Shen, A. W. Lang, G. S. Collider, A. M. Österholm, E. M. Smith, A. L. Tomlinson and J. R. Reynolds, *Chem. Mater.*, 2022, **34**, 1041–1051.

210 M. B. Suarez, C. Aranda, L. Macor, J. Durantini, D. A. Heredia, E. N. Durantini, L. Otero, A. Guerrero and M. Gervaldo, *Electrochim. Acta*, 2018, **292**, 697–706.

211 D. Luo, Y. Zhang, L. Li, C. Shan, Q. Liu, Z. Wang, W. C. H. Choy and A. K. K. Kyaw, *Mater. Today Energy*, 2022, **24**, 100938.

212 M. A. Saeed, S. H. Kim, K. Baek, J. K. Hyun, S. Y. Lee and J. W. Shim, *Appl. Surf. Sci.*, 2021, **567**, 150852.

213 Y. Che, H. Zhang, T. Abdiryim, R. Jamal, A. Kadir, Z. Helil and H. Lui, *Opt. Mater.*, 2021, **122**, 111805.

214 C. Liu, Y. Fu, J. Zhou, L. Wang, C. Guo, J. Cheng, W. Sun, C. Chen, J. Zhou, D. Liu, W. Li and T. Wang, *Adv. Mater.*, 2024, **36**, 2308608.

215 J. Zhou, L. Wang, C. Liu, C. Guo, C. Chen, Y. Sun, Y. Yang, J. Cheng, Z. Gan, Z. Chen, W. Sun, J. Zhou, W. Xia, D. Liu, W. Li and T. Wang, *J. Am. Chem. Soc.*, 2024, **146**, 34998–35006.

216 G. Salinas, A. Villarreal Marquez, M. Idir, S. Shinde, B. A. Frontana-Uribe, M. Raoux, J. Lang, E. Cloutet and A. Kuhn, *Chemelectrochem*, 2020, **7**, 2826–2830.

217 M. Vazquez, J. Bobaka, M. Luostarinen, K. Rissanen, A. Lewenstam and A. Ivaska, *J. Solid State Electrochem.*, 2005, **9**, 312–319.

218 T. Han, Z. Mousavi, U. Mattinen and J. Bobacka, *J. Solid State Electrochem.*, 2020, **24**, 2975–2983.

219 P. Manisankar, C. Vedhi, G. Selvanathan and P. Arumugam, *Microchim. Acta*, 2008, **163**, 289–295.

220 J. M. S. Alshawi, M. Q. Mohammed, H. F. Alesary, H. K. Ismail and S. Barton, *ACS Omega*, 2022, **7**, 20405–20419.

221 G. Salinas, B. A. Frontana-Uribe, S. Reculusa, P. Garrigue and A. Kuhn, *Anal. Chem.*, 2018, **90**, 11770–11774.

222 Y. Sulaiman and R. Kataky, *Analyst*, 2012, **137**, 2386–2393.

223 L. Dong, Y. Zhang, X. Duan, X. Zhu, H. Sun and J. Xu, *Anal. Chem.*, 2017, **89**, 9695–9702.

224 M. Abarkan, A. Pirog, D. Mafilaza, G. Pathak, G. N'Kaoua, E. Puginier, R. O'Connor, M. Raoux, M. J. Donahue, S. Renaud and J. Lang, *Adv. Sci.*, 2022, **9**, 2105211.

225 Y. Liang, A. Offenhäusser, S. Ingebrandt and D. Mayer, *Adv. Healthcare Mater.*, 2021, **10**, 2100061.

226 A. A. Yazza, P. Blondeau and F. J. Andrade, *ACS Appl. Electron. Mater.*, 2021, **3**, 1886–1895.

227 B. D. Paulsen, K. Tybrandt, E. Stavrinidou and J. Rivnay, *Nat. Mater.*, 2020, **19**, 13–26.

228 A. Villarreal Marquez, N. McEvoy and A. Pakdel, *Molecules*, 2020, **25**, 5288.

229 G. E. Fenoy, C. von Bilderling, W. Knoll, O. Azzaroni and W. A. Marmisolle, *Adv. Electron. Mater.*, 2021, **7**, 2100059.

230 S. Carli, M. Di Lauro, M. Bianchi, M. Murgia, A. De Salvo, M. Prato, L. Fadiga and F. Biscarini, *ACS Appl. Mater. Interfaces*, 2020, **12**, 29807–29817.

231 N. Wang, L. Xie, H. Ling, V. Piradi, L. Li, X. Wang, X. Zhu and F. Yan, *J. Mater. Chem. C*, 2021, **9**, 4260.

232 J. Hopkins, K. Fidanovski, L. Travaglini, D. Ta, J. Hook, P. Wagner, K. Wagner, A. Lauto, C. Cazorla, D. Officer and D. A. Mawad, *Chem. Mater.*, 2022, **34**, 140–151.

233 J. Wu, M. Gu, L. Travaglini, A. Lauto, D. Ta, P. Wagner, K. Wagner, E. Zeglio, A. Savva, D. Officer and D. Mawad, *ACS Appl. Mater. Interfaces*, 2024, **16**, 28969–28979.

234 A. L. Jones, M. De Keersmaecker, L. R. Savagian, B. T. DiTullio, I. Pelse and J. R. Reynolds, *Adv. Funct. Mater.*, 2021, **31**, 2102688.

235 L. R. Savagian, A. M. Österholm, J. F. Ponder Jr, K. J. Barth, J. Rivnay and J. R. Reynolds, *Adv. Mater.*, 2018, **30**, 1804647.



236 A. Villarroel Marquez, G. Salinas, M. Abarkan, M. Idir, C. Brochon, G. Hadzioannou, M. Raoux, A. Kuhn, J. Lang and E. Cloutet, *Macromol. Rapid Commun.*, 2020, **41**, 2000134.

237 S. Wustoni, C. Combe, D. Ohayon, M. H. Akhtar, I. McCulloch and S. Inal, *Adv. Funct. Mater.*, 2019, **29**, 1904403.

238 T. Nicolini, S. Shinde, R. El-Attar, G. Salinas, D. Thuau, M. Abbas, M. Raoux, J. Lang, E. Cloutet and A. Kuhn, *Adv. Mater. Interfaces*, 2024, 2400127.

239 G. E. Fenoy, R. Hasler, F. Quartinello, W. A. Marmisolle, C. Lorenz, O. Azzaroni, P. Bäuerle and W. Knoll, *JACS Au*, 2022, **2**, 2778–2790.

240 G. E. Fenoy, C. Lorenz, M. A. Pasquale, W. A. Marmisolle, P. Bäuerle, O. Azzaroni and W. Knoll, *Chem. Mater.*, 2024, **36**, 7207–7221.

241 L. Bouffier, D. Zigah, N. Sojic and A. Kuhn, in *Encyclopedia of Electrochemistry*, ed. A. Bard, Wiley-VCH, Weinheim, Germany, 2022.

242 G. Salinas, S. Arnaboldi, L. Bouffier and A. Kuhn, *Chemelectrochem*, 2022, **9**, e202101234.

243 S. E. Fosdick, K. N. Knust, K. Scida and R. M. Crooks, *Angew. Chem., Int. Ed.*, 2013, **52**, 2–21.

244 K. L. Rahn and R. K. Anand, *Anal. Chem.*, 2021, **93**, 103–123.

245 N. Shida, Y. Zhou and S. Inagi, *Acc. Chem. Res.*, 2019, **52**, 2598–2608.

246 E. O. Bortnikov and S. N. Semenov, *Curr. Opin. Electrochem.*, 2022, **35**, 101050.

247 G. Salinas and A. Kuhn, *Curr. Opin. Electrochem.*, 2025, **49**, 101612.

248 Z. Qi, S. You and N. Ren, *Electrochim. Acta*, 2017, **229**, 96–101.

249 L. Bouffier, D. Zigah, N. Sojic and A. Kuhn, *Annu. Rev. Anal. Chem.*, 2021, **14**, 65–86.

250 Y. Koizumi, N. Shida, M. Ohira, H. Nishiyama, I. Tomita and S. Inagi, *Nat. Commun.*, 2016, **7**, 10404.

251 M. Ohira, Y. Koizumi, H. Nishiyama, I. Tomita and S. Inagi, *Polym. J.*, 2017, **49**, 163–167.

252 Y. Koizumi, M. Ohira, T. Watanabe, H. Nishiyama, I. Tomita and S. Inagi, *Lagmuir*, 2018, **34**, 7598–7603.

253 T. Watanabe, M. Ohira, Y. Koizumi, H. Nishiyama, I. Tomita and S. Inagi, *ACS Macro Lett.*, 2018, **7**, 551–555.

254 N. Shida, T. Watanabe, I. Tomita and S. Inagi, *Synth. Met.*, 2020, **266**, 116439.

255 Y. Zhou, N. Shida, Y. Koizumi, T. Watanabe, H. Nishiyama, I. Tomita and S. Inagi, *J. Mater. Chem. C*, 2019, **7**, 14745.

256 E. Villani, Y. Zhang, Z. Chen, Y. Zhou, M. Konishi, I. Tomita and S. inagi, *ACS Appl. Polym. Mater.*, 2023, **5**, 6186–6198.

257 E. Villani, N. Shida and S. Inagi, *Electrochim. Acta*, 2021, **389**, 138718.

258 A. Brady, M. Wagner and R. J. Forster, *Chem. Commun.*, 2024, **60**, 13000.

259 M. Wagner, A. Brady, O. F. Doyle and R. J. Forster, *Chemelectrochem*, 2025, **12**, e202400506.

260 A. Brady and R. J. Forster, *Anal. Chem.*, 2025, **97**, 410–418.

261 T. Nicolini, Y. Boukarkour, S. Reculusa, N. Sojic, A. Kuhn and G. Salinas, *Electrochim. Acta*, 2023, **458**, 142506.

262 H. Jin, K. Kim, S. Park, J. H. Rhee, H. Ahn, D. J. Kim, K. Kim, J. H. Noh, T. S. Kim, E. Y. Shin and H. J. Son, *Adv. Funct. Mater.*, 2023, **33**, 2304930.

263 N. Nozaki, A. Uva, H. Matsumoto, H. Tran and M. Ashizawa, *RSC Appl. Polym.*, 2024, **2**, 163–171.

264 D. Mantione, I. del Agua, A. Sanchez-Sanchez and D. Mecerreyes, *Polymers*, 2017, **9**, 354.

265 A. Emin, A. Ding, S. Ali, M. Chhattal, S. Ali, A. Parkash and Q. Li, *Microchem. J.*, 2024, **207**, 111972.

266 J. Gao, K. Yu, Q. Luo, M. Deng, X. Hou, W. Wang, X. Zeng, X. Xiong, Y. He, X. Hong and Y. Xiao, *J. Med. Chem.*, 2024, **67**, 12428–12438.

267 J. Gao, H. Zhu, H. Cai, Q. Ding, X. Xiong, T. Zhang, B. Chen, W. Wang, X. Ju, J. Huang, X. Zeng, J. S. Kim and X. Hong, *Chem. Eng. J.*, 2025, **503**, 158455.

268 F. Tian, J. Yu, W. Wang, D. Zhano, J. Cao, Q. Zhano, F. Wang, H. yanhg, Z. Wu, J. Xu and B. Lu, *J. Colloid Interface Sci.*, 2023, **638**, 339–348.

269 D. Liu, C. Huyan, Z. Wang, Z. Guo, X. Zhang, H. Torun, D. Mulvihill, B. B. Xu and F. Chen, *Mater. Horiz.*, 2023, **10**, 2800–2823.

270 H. Wang, X. liu, C. Ling, Z. Shen and M. Li, *React. Funct. Polym.*, 2025, **214**, 106300.

271 Y. Zhang, R. Jamal, S. Xie, A. Abdurexit, T. Abdiryim, Y. Zhang, Y. Song and Y. Liu, *J. Colloid Interface Sci.*, 2024, **659**, 235–247.

272 B. Nemutlu, E. F. Eker, A. M. Önal, E. G. C. Ergun and C. Tanyeli, *ACS Omega*, 2025, **10**, 29442–29451.

273 A. C. Da Silva, X. Hu, V. H. Paschoal, N. Hagis, A. J. Zajac, M. C. C. Ribeiro and I. R. Minev, *Commun. Mater.*, 2025, **6**, 28.

274 C. Qin, Z. Yue, X. F. Huang, R. J. Forster, G. G. Wallace and J. Chen, *Appl. Mater. Today*, 2022, **27**, 101481.

275 T. A. Skotheim and J. Reynolds ed. *Handbook of Conducting Polymers*, CRC Press, Boca Raton, USA, 3<sup>rd</sup> edn, 2007.

